NUREG/IA-0249

International Agreement Report

Loss of External Load Analysis with RELAP5/MOD3.3 Patch 03 Code

Prepared by:
A. Prošek, B. Mavko

Jožef Stefan Institute
Jamova cesta 39
SI-1000 Ljubljana, Slovenia

A. Calvo, NRC Project Manager

Office of Nuclear Regulatory Research
U.S. Nuclear Regulatory Commission
Washington, DC 20555-0001

December 2010

Prepared as part of
The Agreement on Research Participation and Technical Exchange
Under the International Code Assessment and Maintenance Program (CAMP)

Published by
U.S. Nuclear Regulatory Commission

AVAILABILITY OF REFERENCE MATERIALS IN NRC PUBLICATIONS

NRC Reference Material

As of November 1999, you may electronically access NUREG-series publications and other NRC records at NRC's Public Electronic Reading Room at http://www.nrc.gov/reading-rm.html. Publicly released records include, to name a few, NUREG-series publications; *Federal Register* notices; applicant, licensee, and vendor documents and correspondence; NRC correspondence and internal memoranda; bulletins and information notices; inspection and investigative reports; licensee event reports; and Commission papers and their attachments.

NRC publications in the NUREG series, NRC regulations, and *Title 10, Energy*, in the *Code of Federal Regulations* may also be purchased from one of these two sources.

1. The Superintendent of Documents
   U.S. Government Printing Office
   Mail Stop SSOP
   Washington, DC 20402-0001
   Internet: bookstore.gpo.gov
   Telephone: 202-512-1800
   Fax: 202-512-2250
2. The National Technical Information Service
   Springfield, VA 22161-0002
   www.ntis.gov
   1-800-553-6847 or, locally, 703-605-6000

A single copy of each NRC draft report for comment is available free, to the extent of supply, upon written request as follows:

Address: U.S. Nuclear Regulatory Commission
Office of Administration
Mail, Distribution and Messenger Team
Washington, DC 20555-0001
E-mail: DISTRIBUTION@nrc.gov
Facsimile: 301-415-2289

Some publications in the NUREG series that are posted at NRC's Web site address http://www.nrc.gov/reading-rm/doc-collections/nuregs are updated periodically and may differ from the last printed version. Although references to material found on a Web site bear the date the material was accessed, the material available on the date cited may subsequently be removed from the site.

Non-NRC Reference Material

Documents available from public and special technical libraries include all open literature items, such as books, journal articles, and transactions, *Federal Register* notices, Federal and State legislation, and congressional reports. Such documents as theses, dissertations, foreign reports and translations, and non-NRC conference proceedings may be purchased from their sponsoring organization.

Copies of industry codes and standards used in a substantive manner in the NRC regulatory process are maintained at—

The NRC Technical Library
Two White Flint North
11545 Rockville Pike
Rockville, MD 20852-2738

These standards are available in the library for reference use by the public. Codes and standards are usually copyrighted and may be purchased from the originating organization or, if they are American National Standards, from—

American National Standards Institute
11 West 42nd Street
New York, NY 10036-8002
www.ansi.org
212-642-4900

Legally binding regulatory requirements are stated only in laws; NRC regulations; licenses, including technical specifications; or orders, not in NUREG-series publications. The views expressed in contractor-prepared publications in this series are not necessarily those of the NRC.

The NUREG series comprises (1) technical and administrative reports and books prepared by the staff (NUREG-XXXX) or agency contractors (NUREG/CR-XXXX), (2) proceedings of conferences (NUREG/CP-XXXX), (3) reports resulting from international agreements (NUREG/IA-XXXX), (4) brochures (NUREG/BR-XXXX), and (5) compilations of legal decisions and orders of the Commission and Atomic and Safety Licensing Boards and of Directors' decisions under Section 2.206 of NRC's regulations (NUREG-0750).

NUREG/IA-0249

Loss of external load analysis with RELAP5/MOD3.3 Patch 03 code

Manuscript Completed: September 2010
Date Published: December 2010

Prepared by: Andrej Prošek, Borut Mavko

Jožef Stefan Institute
Jamova cesta 39
SI-1000 Ljubljana, Slovenia

A. Calvo, NRC Project Manager

Prepared as part of
The Agreement on Research Participation and Technical Exchange
Under the International Code Assessment and Maintenance Program (CAMP)

Office of Nuclear Regulatory Research
U.S. Nuclear Regulatory Commission
Washington, DC 20555-0001

ABSTRACT

By removing resistance temperature detectors (RTD) bypass manifold system with fast-response thermowell-mounted RTDs the reactor coolant system temperature measurement time may change, what influences the time delays for overtemperature ΔT (OTΔT) and overpower ΔT (OPΔT) trips. The total time delays should not exceed the value assumed in the accident analyses.

In this paper we are presenting Krško nuclear power plant specific analysis of loss of external load varying the total delay time for OTΔT trip. For simulations the latest RELAP5/MOD3.3 Patch 03 thermal hydraulic computer code was used. The verified standard RELAP5/MOD3.3 input model from 2008 (cycle 23) was delivered by Krško nuclear power plant. Base case calculation was compared to safety analysis report calculation to qualify the RELAP5 calculated results before the sensitivity analyses were performed.

CONTENTS

Figures

Tables

EXECUTIVE SUMMARY

Several nuclear power plants remove resistance temperature detectors (RTD) bypass manifold system with fast-response thermowell-mounted RTDs. The reactor coolant system temperature measurement time may therefore change, what influences the total response time for overtemperature ΔT (OTΔT) and overpower ΔT (OPΔT) trip signals. The total response time should not exceed the time delay for trip assumed in the accident analyses. The objective of this study was to investigate the influence of measurement delay on OTΔT trip protection during loss of external load analysis. For simulations the latest RELAP5/MOD3.3 Patch 03 thermal hydraulic computer code was used. The verified standard RELAP5/MOD3.3 input model from 2008 (cycle 23) was delivered by Krško nuclear power plant. First comparison with the original updated safety analysis report (USAR) calculation was done to show that main plant parameters agree with USAR calculation and that the quantitative differences are understood. The differences were mainly due to different computer codes, as the code used for USAR calculation was not best-estimate code. Then sensitivity analyses were performed. The results showed that when the temperature measurement delay was rather small (e.g. ± 2 seconds of the value assumed in USAR), also the trip time on OTΔT was similarly delayed. The study also demonstrated that the trends for departure from nuclear boiling ratio can be evaluated by RELAP5/MOD3.3 Patch 03 using the critical heat flux ratio for the average core condition, while for the licensing calculation of minimum DNBR the coupling of RELAP5 code with the code having capability to calculate transient DNBR for hot rod is required, taken into account local mass flux and local quality.

ACKNOWLEDGEMENTS

The authors acknowledge the financial support from Krško Nuclear Power Plant and Slovenian Nuclear Safety Administration within CAMP program (project no. POG-3473) and from the state budget by the Slovenian Research Agency (program no. P2-0026). The RELAP5/MOD3.3 base input model of Krško nuclear power plant is the courtesy of Krško Nuclear Power Plant. Finally, special thanks to M.Sc. Božidar Krajnc, director of engineering services division in Krško nuclear power plant, for expressing the need for such an analysis and for permission to publish the results from updated safety analysis report.

ABBREVIATIONS

ACC	accumulator
AFW	auxiliary feedwater
AP1000	advanced passive 1000
CHFR	critical heat flux ratio
CPU	central processing unit
CVCS	chemical and volume control system
DNB	departure from nucleate boiling
DNBR	departure from nucleate boiling ratio
ECCS	emergency core cooling system
HPSI	high-pressure safety injection
I&B	initial and boundary
LPSI	low-pressure safety injection
MD	motor driven
MFW	main feedwater
MPa	megapascal
MWt	megawatt thermal
NPP	nuclear power plant
OPΔT	overpower delta T
OTΔT	overtemperature delta T
PORV	power operated relief valve
PRZ	pressurizer
PWR	pressurized water reactor
RCP	reactor coolant pump
RCS	reactor coolant system
RPV	reactor pressure vessel
RTD	resistance temperature detector
SG	steam generator
SL	surge line
TD	turbine driven
USAR	updated safety analysis report

1. INTRODUCTION

Several nuclear power plants remove resistance temperature detectors (RTD) bypass manifold system with fast-response thermowell-mounted RTDs. The total response time for overtemperature ΔT (OTΔT) and overpower ΔT (OPΔT) may affect the accident analyses. Fast acting RTD/thermowell response time is slower than response of direct immersion RTD, but there is no loop transport or thermal lag. Depending on the delay of fast acting RTD, new analysis may be needed or not. The total response time for OTΔT is specified in the plant technical specifications. When new total response time is bounded by technical specification response time, safety analyses are not affected. The influence of measurement delay on departure from nucleate boiling (DNB), which is protected by OTΔT trip, was investigated for the selected loss of external load transient. For simulations the latest RELAP5/MOD3.3 Patch 03 thermal hydraulic computer code was used. The verified standard RELAP5/MOD3.3 input model from 2008 (cycle 23) was delivered by Krško nuclear power plant. The analysis focused on the DNB, while overpressure analysis is not influenced by OTΔT response time.

The core average DNBR is not a safety related item as it is not directly related to minimum DNBR in the core, which occurs at some elevation in the limiting flow channel. Similarly, the DNBR at the hot spot is not directly related. The minimum DNBR in the limiting flow channel will be downstream of the peak heat flux location (hot spot) due to the increased downstream enthalpy. The LOFTRAN computer code, which was used in the updated safety analysis report (USAR) analysis, has the capability of calculating transient value of DNBR. On the other hand, the RELAP5 is limited to calculate the departure from nucleate boiling ratio (DNBR). Also, the study assessing the CHF predictive methods accessible in the open literature, including RELAP5 methods, showed that no satisfactory model to predict critical heat flux for non-uniform heat flux exists (Ref. 1). In RELAP5 the heat transfer critical heat flux ratio (CHFR) can be obtained by division of critical heat flux by heat transfer coefficient during subcooled or saturated boiling. This ratio has been added to the list of plot variables in the RELAP5/MOD3.3. The hot spot was modeled by hot rod to evaluate the DNBR trend by RELAP5/MOD3.3. The purpose of the study was to perform sensitivity analysis by varying temperature measurement delay ± 2 seconds. To confirm the correct trend of DNBR evaluation, first comparison of RELAP5 results with the results from the original USAR analysis was done to show that main plant parameters including DNBR trend agree and that the quantitative differences are understood.

2. PLANT DESCRIPTION

Krško NPP is a Westinghouse two-loop pressurized-water reactor (PWR) plant with a large dry containment. The plant has been in commercial operation since 1983. After modernization in 2000, the plant's fuel cycle was gradually prolonged from 12 (cycle 17) to 18 months (cycle 21).

The power rating of the Krško NPP nuclear steam supply system is 2,000 megawatt thermal (MWt) (1,882 MWt before the plant modernization and power uprate), comprising 1,994 MWt (1,876 MWT before the plant modernization and power uprate) of core power output plus 6 MWt of reactor coolant pumps (RCPs) heat input. The reactor coolant system (RCS) is arranged as two closed reactor coolant loops connected in parallel to the reactor vessel, each containing an RCP and a steam generator (SG). An electrically heated pressurizer is connected to one of the loops.

The reactor core is composed of 121 fuel assemblies. The RCPs, one per coolant loop, are Westinghouse vertical, single-stage, centrifugal pumps of the shaft-seal type. The SGs, one per loop, are vertical U-tube, Siemens-Framatome type SG 72 W/D4-2 units, installed during the plant modernization in 2000.

For more detailed description of the plant the reader is referred to Ref. 2.

3. INPUT MODEL DESCRIPTION

To perform the analysis, Krško NPP has provided the base RELAP5 input model, so called "Master input deck", which have been used for several analyses, including reference calculations for Krško full scope simulator verification (Refs. 3, 4, 5). The analysis was performed for uprated conditions (2000 MWt) with new steam generators (SGs) and Cycle 23 settings, corresponding to the expected plant state after outage and refueling in October 2007.

The model consists of 469 control volumes, 497 junctions and 378 heat structures with 2107 radial mesh points. The nodalization scheme of Krško NPP for RELAP5 it is shown in Figure 1. The scheme was generated by SNAP through importing ASCII input deck and then manually rearranging the position and size of the volumes and junctions.

Modeling of the primary side without the reactor vessel and both loops includes the pressurizer (PRZ) vessel, pressurizer surge line (SL), pressurizer spray lines and valves, two pressurizer power operated relief valves (PORVs) and two pressurizer safety valves, chemical and volume control system (CVCS) charging and letdown flow, and RCP seal flow. The reactor vessel (RPV) consists of the lower downcomer, lower head, lower plenum, core inlet, reactor core, core baffle bypass, core outlet, upper plenum, upper head, upper downcomer, and guide tubes. The primary loop is represented by the hot leg, primary side of the steam generator (SG), intermediate leg with cold leg loop seal, and cold leg, separately for loop 1 and loop 2. Loops are symmetrical except for the pressurizer surge line and the chemical and volume control system connections layout. The primary side of the SG consists of the inlet and outlet plenum, tubesheet, and the U-tube bundle represented by a single pipe. Emergency core cooling system (ECCS) piping includes high-pressure safety injection (HPSI) pumps, accumulators (ACCs), and low-pressure safety injection (LPSI) pumps.

The secondary side consists of the SG secondary side (riser, separator and separator pool, downcomer, steam dome), main steamline, main steam isolation valves (MSIVs), SG relief and safety valves, main feedwater (MFW) piping, and auxiliary feedwater (AFW) piping from the header to the SG. The AFW injects above the SG riser. The main steam no. 1 has same volumes as main steam no. 2, but the geometry data differ depending on pipeline. Turbine valve is modeled by the corresponding logic, while turbine is represented by time dependent volume. MFW and AFW pumps are modeled as time dependent junctions, pumping water from time dependent volumes, representing the condensate storage tank. For AFW pumps (two motor driven and one turbine driven), recirculation flow is modeled too.

In order to accurately represent the Krško NPP behavior, a considerable number of control variables and general tables are part of the model. They represent protection, monitoring and simplified control systems used only during steady state initialization, as well as the following main plant control systems: (a) rod control system, (b) PRZ pressure control system, (c) PRZ level control system, (d) SG level control system, and (e) steam dump. It must be noted that rod control system has been modeled for point kinetics. The reactor protection system was based on trip logic. It includes reactor trip signal, safety injection signal, turbine trip signal, steam line isolation signal, MFW isolation signal, and AFW start signal.

For further details of the above mentioned plant systems and components, plant signals and control systems schemes the reader can refer to Reference 2.

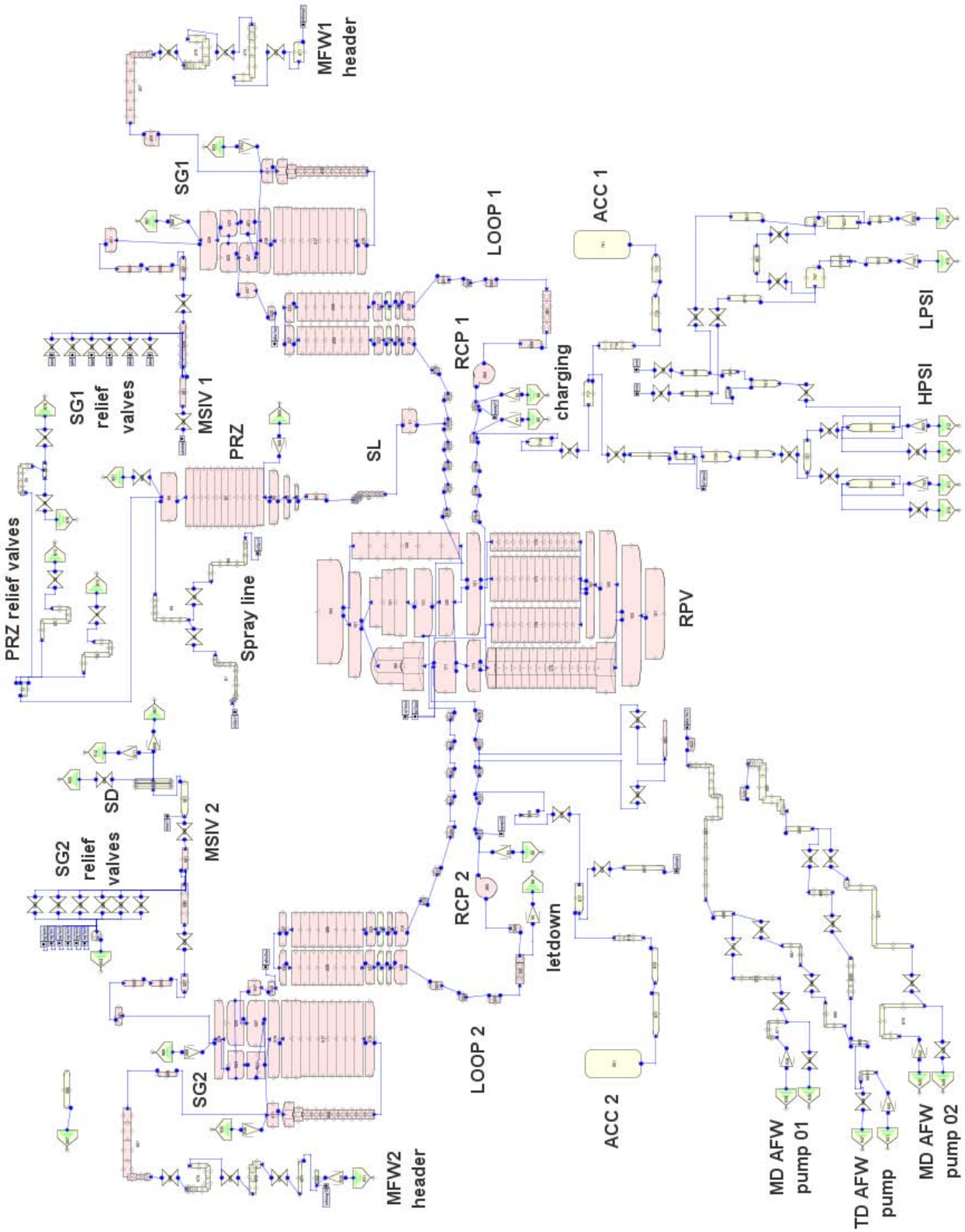

Figure 1 Krško NPP nodalization scheme – SNAP hydraulics component view

4. SCENARIO DESCRIPTION

Loss of load can result from loss of external electrical load due to some electrical system disturbance. Offsite power remains available to operate plant components such as the reactor coolant pumps. Following the loss of generator load, the turbine stop valves immediately close. This causes sudden reduction in steam flow, resulting in increase in the temperature and pressure in the steam generator. Heat transfer rate is reduced, causing the reactor coolant temperature to increase, which in turn causes reactor coolant expansion, pressurizer insurge and primary pressure rise. For loss of load without subsequent turbine trip, no direct reactor trip would be generated, since the plant has full load rejection capability. The plant is expected to trip from the reactor protection system signals (pressurizer pressure high, pressurizer water level high, overtemperature ΔT, overpower ΔT and steam generator water level low-low). It is assumed that plant auxiliary loads require 5% steam flow. Since the reactor trip on turbine trip is not credited and the steam dump fails by assumption, the primary and secondary side pressure increase is protected by pressurizer and steam generator safety valves.

The main conservative assumptions in the USAR analysis, which leads to the minimum departure from boiling ratio (DNBR), were the following:

- reactor trip on high pressurizer pressure setpoint increased (to delay reactor trip),
- reactor trip on turbine trip is not credited (reactor trip on other signal is later),
- steam dump system not credited (failure of steam dump system could lead to a significant increase in a secondary side pressure and a heatup of the primary side),
- rod control system not credited (to increase heatup and maximize power),
- steam generator power operated relief valves not credited (to increase a secondary side pressure and a heatup of the primary side),
- feedwater flow follows 5% steam flow until reactor trip (this adds considerably less feedwater than in reality when SG level control would attempt to compensate for water level decrease so the cooldown is minimized),
- pressurizer pressure control assumed to function (to delay reactor trip and to minimize pressure for DNB calculation - pressurizer spray and PORVs reduce or limit the pressure, while pressurizer heaters are not simulated),
- minimum reactivity feedback (to slowdown the power decrease),
- high RCS average temperature case, 5% plugging level (less subcooling, smaller mass flow).

In the first phase (base case analysis), the loss of external load analysis with the same initial and boundary conditions (see Table 1), and assumptions as specified above was analyzed. In general the initial conditions agree well. Due to different code and geometry, there was some difference in the secondary pressure. The aim of this analysis was to compare RELAP5 calculations using NPP Krško standard input deck against USAR calculation to find possible differences in response due to different geometry (known for pressurizer water volume and steam generator mass) and the computer code (note that LOFTRAN code is not a best-estimate code). The modeling simplifications in LOFTRAN are such that they are conservative for safety analysis. The base case scenario was performed with compensation of heat transfer on the primary side in order to as closely as possible to reproduce the USAR primary pressure and temperature increase, at which DNBR was calculated. In this way the conditions for DNBR evaluation were similar to the USAR conditions with limitation that local conditions in hot channel were not considered in the RELAP5 (local mass flow and local quality).

Table 1 Comparison between USAR and RELAP5 initial conditions

Variable	USAR	RELAP5	remark
Nuclear steam supply system power (MW)	2000	2000	
RCS average temperature (K)	580.39	580.39	high T_{avg}
Minimum measured flow (per loop) m^3/h	6.151	6.151	5% plugging
Pressurizer pressure (MPa)	15.513	15.513	
Pressurizer water volume (m^3)	18.2	18.4	correspond to 67% level (with 5% uncertainty)
Steam generator pressure (MPa)	6.46	6.64	
Steam flow (kg/s)	1090	1090	
Feedwater temperature (K)	565.55	565.55	constant
Steam generator mass (per SG) (kg)	42210	44350	90% of nominal

In the second phase, the sensitivity analyses were performed to study the influence of temperature measurement time delay on OTΔT signal causing reactor trip and DNBR evaluation by CHFR. In order to study temperature measurement delay on OTΔT signal, the reactor trip on high pressurizer pressure and high pressurizer level were disabled. It should be pointed out that such scenarios are not much probable and are not analyzed in the safety analysis reports.

Three different cases were considered in which the temperature measurement delay was varied ± 2 seconds from the nominal delay: a) case 1 using same initial and boundary conditions as in the base case with primary side heat transfer compensation, b) case 2 being same as the case 1 except that best estimate sprays flow and PORVs flow were considered (i.e. no primary side heat transfer compensation), including one pressurizer PORV to be rate sensitive like in the plant, and c) case 3 being same as case 2 except that normal measured reactor coolant system flow and pressurizer level were considered (6.22 m^3/h and 62%). It should be noted that base case scenario was compensated for the reason of different codes. Therefore case 2 was analyzed having no such compensation. Finally, the case 3 was performed by normal measured flow to see its influence on the results.

5. RESULTS

5.1 Base Calculation

The results of base case RELAP5 calculation compared to USAR calculation are shown in Figures 2 through 11. For DNBR calculation the initial 20 s are important. Figures show that the main variables of base case calculation qualitatively and quantitatively agree well with the USAR calculation. As the LOFTRAN is conservative code, in the RELAP5 calculation the conservatism in the primary side heatup was compensated by reduced cooling of the primary side to get quantitative agreement in the initial period of 20 s, when minimum DNBR occurs. Similar conservatism existed also for the secondary side heatup due to reduced steam flow, but no compensation was made because by steam generator relief valves initially such compensation is not feasible. Later, after minimum DNBR occurrence (slightly after reactor trip, see Figure 2) heat transfer on the secondary side has no more influence on minimum DNBR calculation. The heat transfer on the primary side was compensated on the primary side by reduced spray and pressurizer PORVs flow to be more conservative in RCS heatup (in the opposite no reactor trip on high pressurizer pressure would be generated and the transient progression would be different - the reactor would trip on high pressurizer level). In the period with no discharge through pressurizer relief valves and spray flow (after 17 s), the compensation is no more present and the RELAP5 calculated pressurizer pressure drops more slowly than in USAR analysis, as can be seen from Figure 3. Also in the RCS temperature differences occurs in the period with no heat transfer compensation. Faster cooling in the RELAP5 case causes contraction of coolant in the pressurizer (see Figure 4). The reactor coolant system average temperature, the hot leg temperature and the cold leg temperature are shown in Figures 5, 6 and 7, respectively. The rate of temperature increase is similar due to compensation. Nevertheless, in the USAR calculation the temperature started to increase earlier and this is attributed to the computer code. The reduced pressurizer PORVs flow can be seen from Figure 8 showing pressurizer relief valves flow. First discharge comes from PORVs with flow rate around 38 kg/s, while spike indicates safety valves opening. On the secondary side no heat transfer compensation was made, therefore conservative code used in USAR analysis causes faster secondary pressure increase, which is shown in Figure 9. The differences in the secondary side relief valves flow and closure time (see Figure 10) influence the later period of analysis. The focus of the analysis was to reproduce the initial phase until minimum DNBR is reached. Finally, Figure 11 comparing DNBR and CHFR shows that LOFTRAN and RELAP5 trends are quite similar. It should be noted that the values could not be compared directly as CHFR was based on RELAP5 lookup table and minimum CHFR limit is not known like minimum DNBR limit in USAR calculation. However, the trends may give us some information in the sensitivity analysis of temperature measurement delay. Finally, during transient in total around 20% of DNBR margin was lost in USAR calculation comparing to DNBR margin in normal operation.

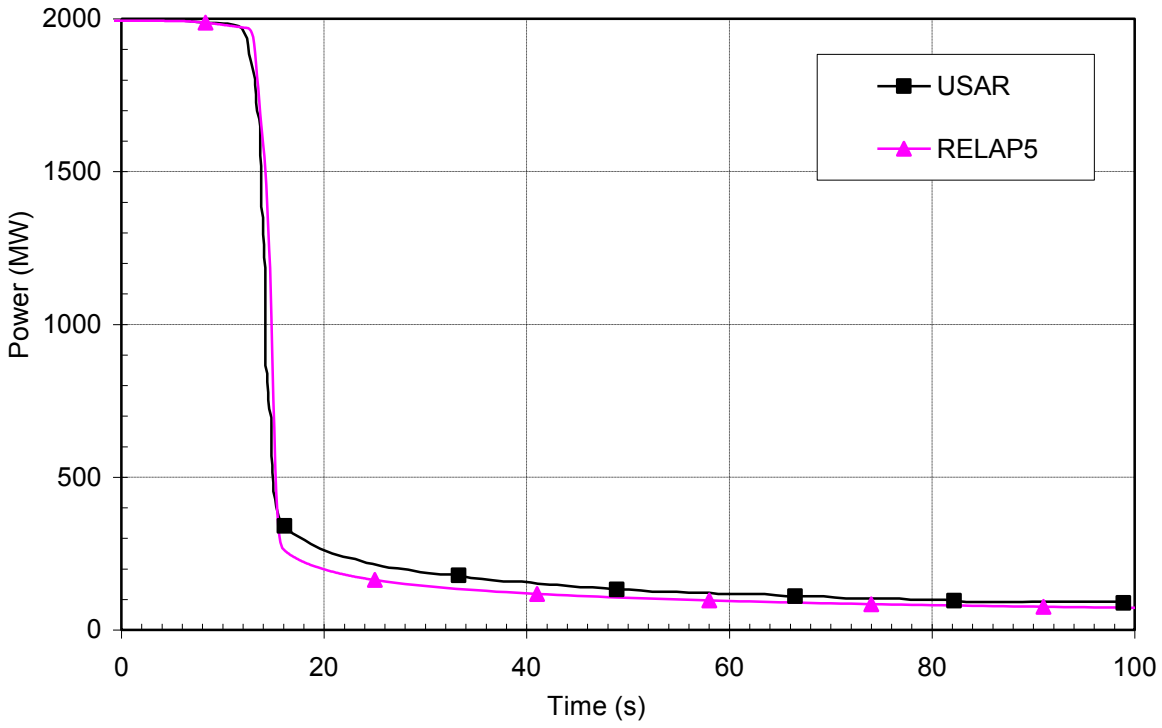

Figure 2 Reactor power - base case comparison between RELAP5 and USAR

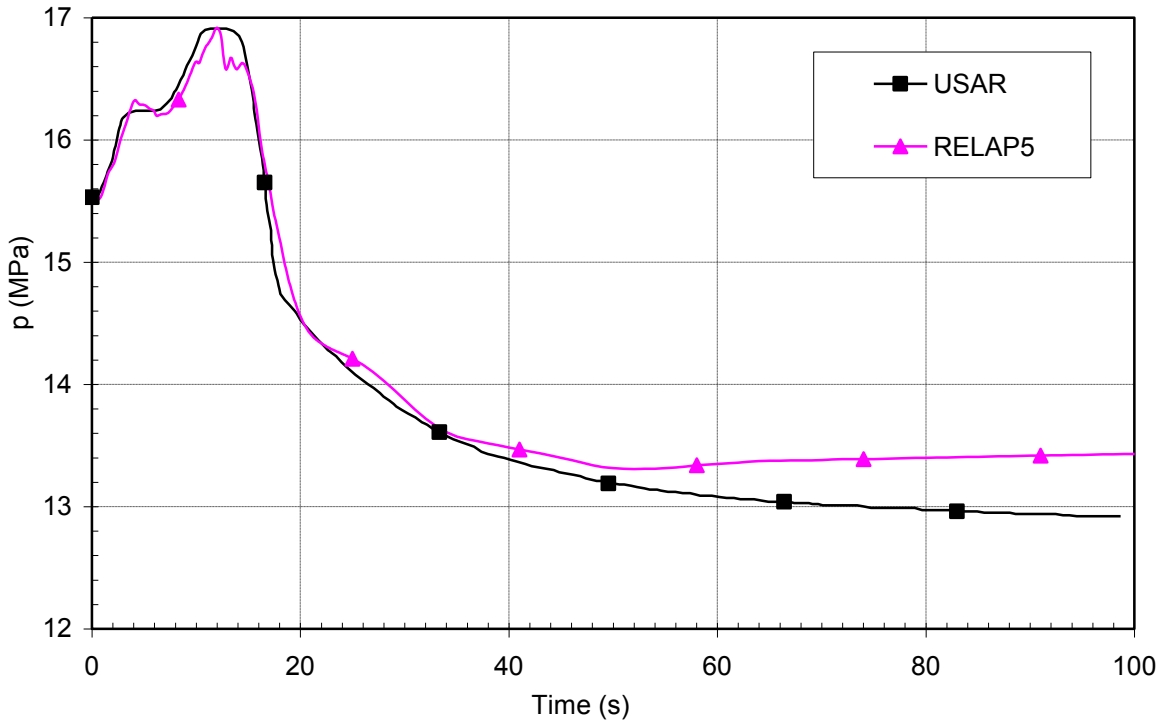

Figure 3 Pressurizer pressure - base case comparison between RELAP5 and USAR

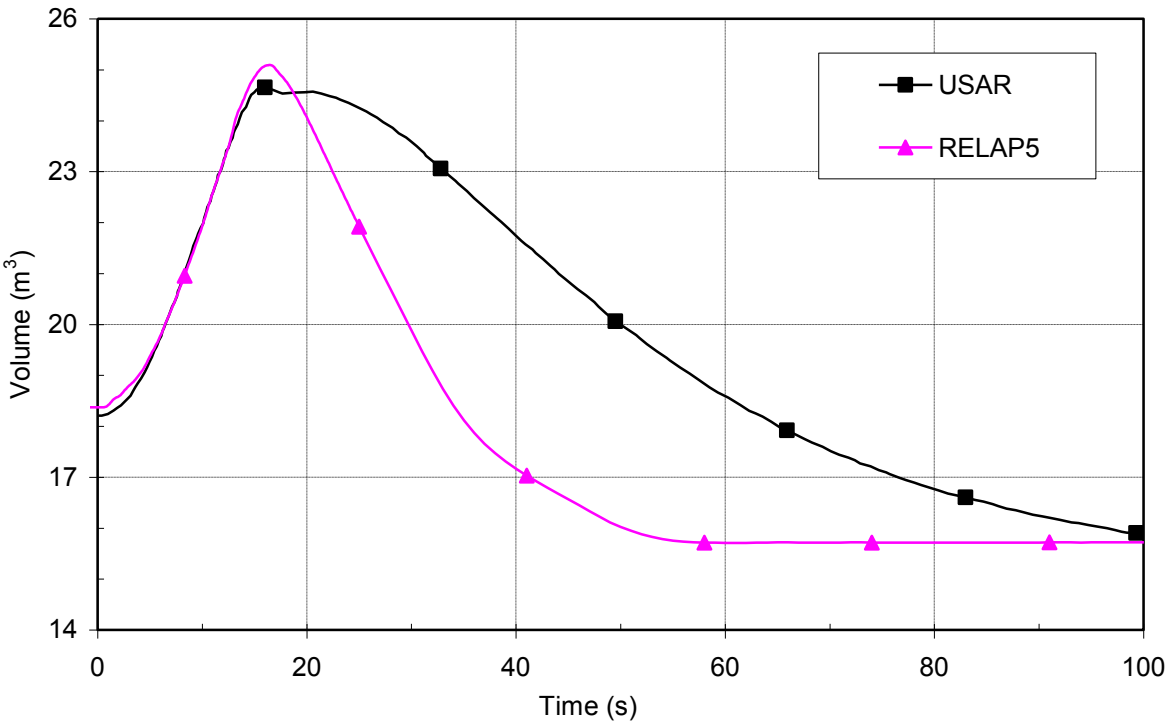

Figure 4 Pressurizer volume - base case comparison between RELAP5 and USAR

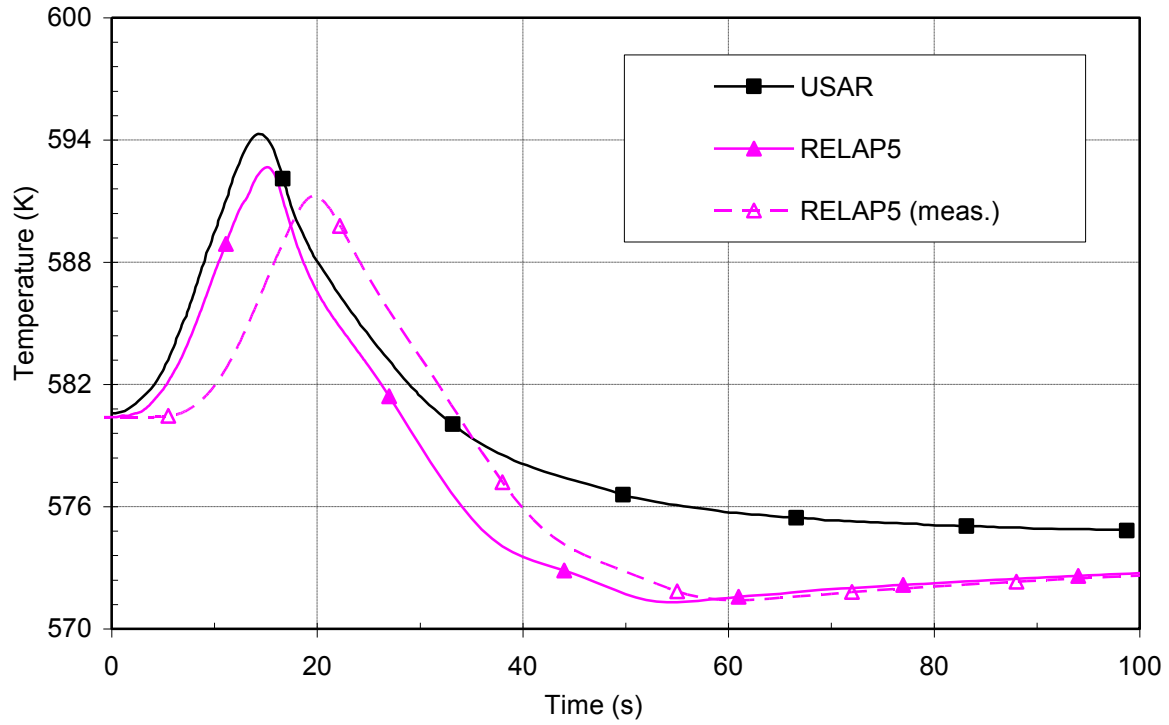

Figure 5 RCS average temperature and measured RCS average temperature - base case comparison between RELAP5 and USAR

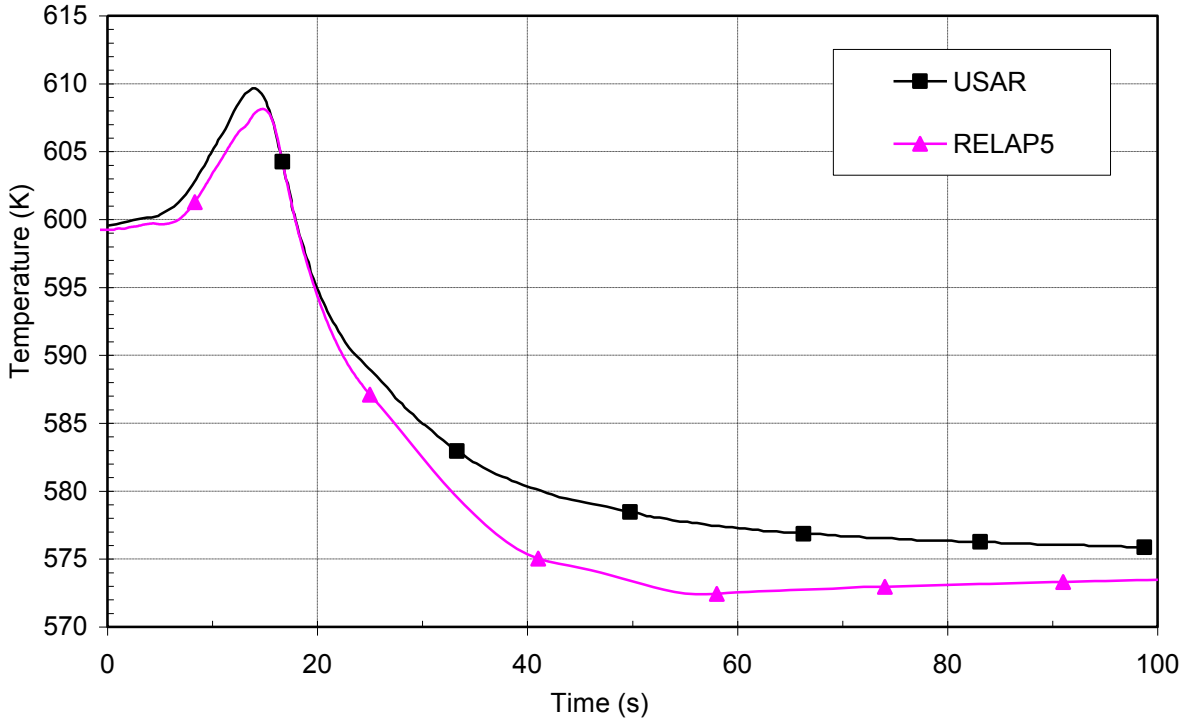

Figure 6 Hot leg no. 1 temperature - base case comparison between RELAP5 and USAR

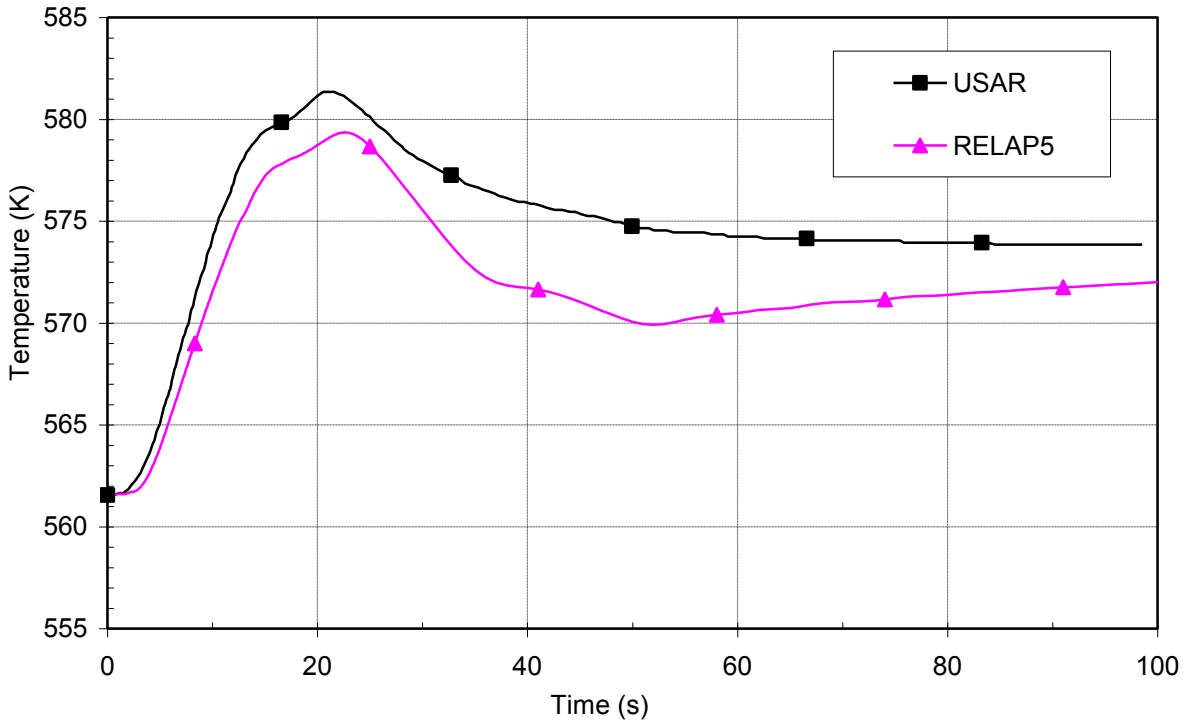

Figure 7 Cold leg no. 1 temperature - base case comparison between RELAP5 and USAR

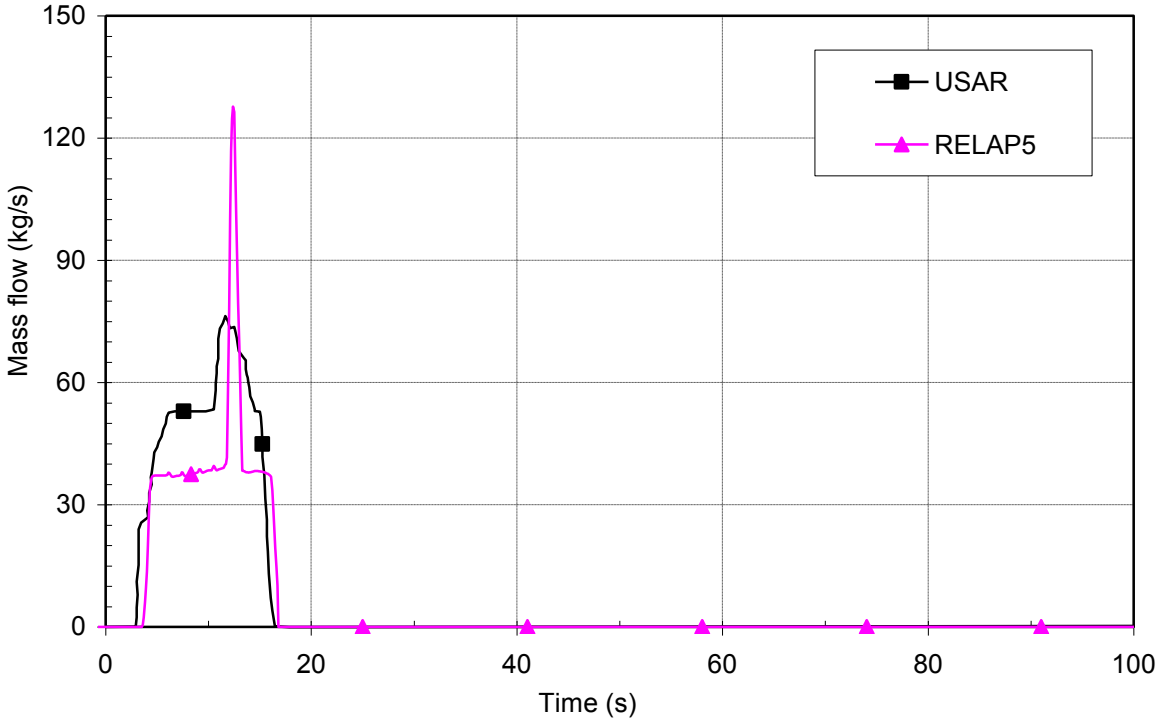

Figure 8 Pressurizer relief valves flow - base case comparison between RELAP5 and USAR

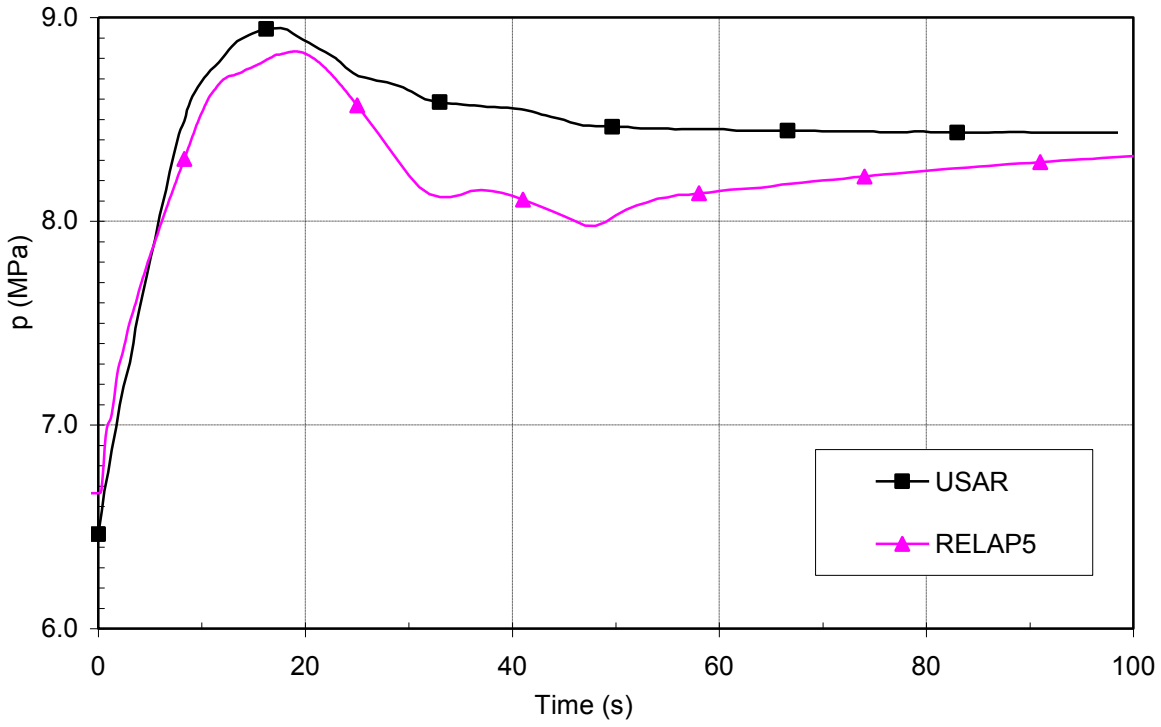

Figure 9 Steam generator no. 1 pressure - base case comparison between RELAP5 and USAR

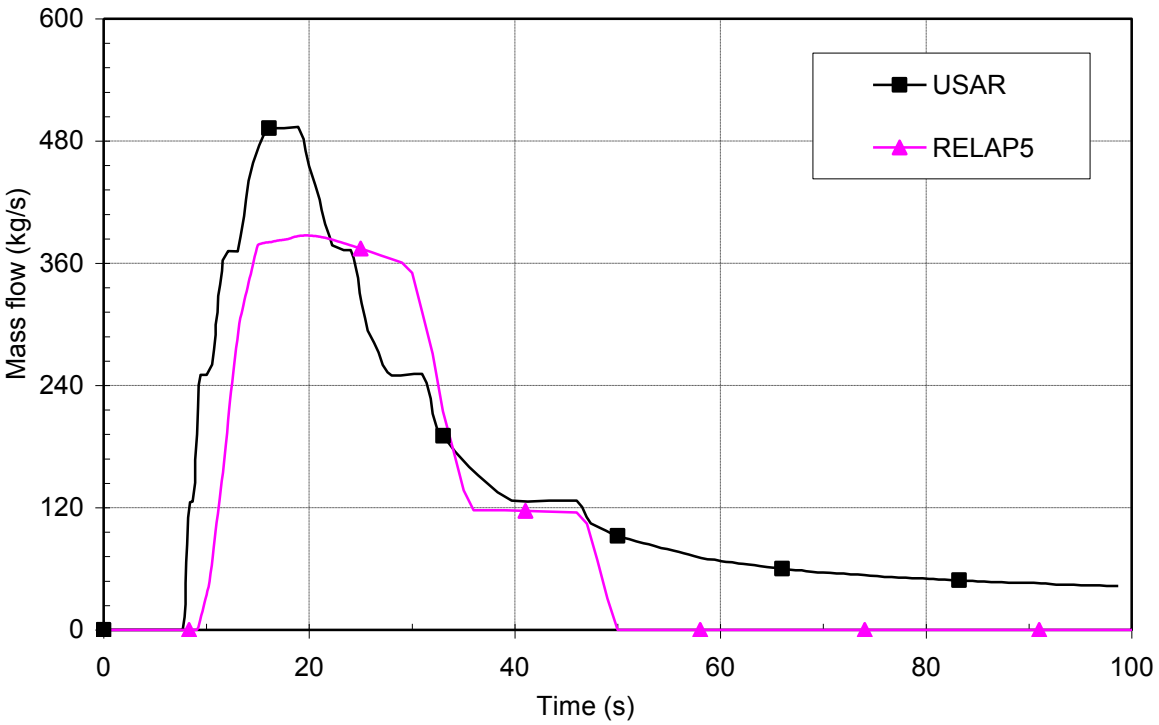

Figure 10 Steam generator no. 1 relief valves mass flow - base case comparison between RELAP5 and USAR

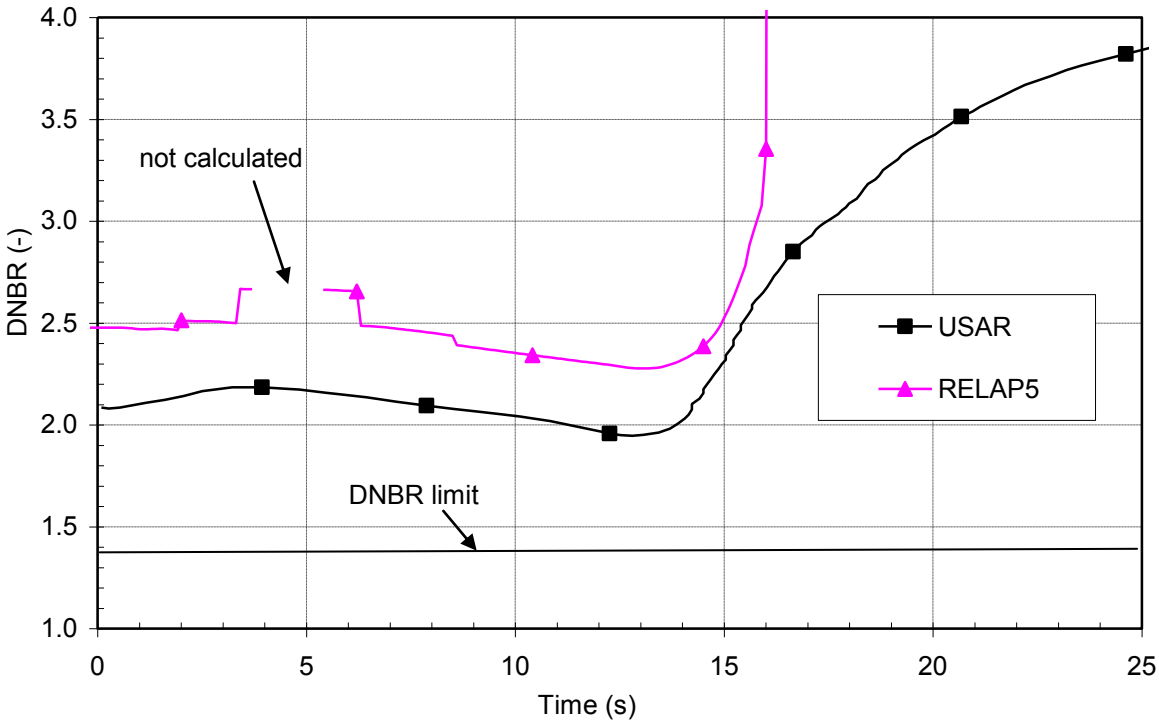

Figure 11 Departure from nucleate boiling ratio (critical heat flux ratio) - base case comparison between RELAP5 and USAR

5.2 Sensitivity Calculations

In the Figures 12 through 24 three cases were compared, in which initial and boundary conditions were varied while the measurement delay was for the existent RTD (total delay time of OTΔT trip signal is less than 6 s assumed in the safety analysis). Then for each case the measurement delay time was varied ± 2 seconds (representing the analyses with total delay time of OTΔT trip signal of 4 and 8 seconds to be assumed in the safety analysis). The influence of temperature measurement delay on parameters used for CHFR calculation, OTΔT trip signal and CHFR calculation is shown in Figures 25 through 33, Figures 34 through 42, and Figures 43 through 51 for case 1, case 2 and case 3, respectively. Finally, Table 2 shows sensitivity of OTΔT trip time and minimum CHFR on RCS temperature measurement response time.

5.2.1 Variation of Initial and Boundary Conditions

The reactor power shown in Figure 12 shows, that OTΔT reactor trip signal in the case 1 with reduced spray and PORV flow occurs later than in the cases 2 and 3 assuming best-estimate spray and PORVs flow. The reason is the higher pressure (see Figure 13) which is less conservative for CHFR calculation. The differences in the pressure are due to best estimate modeling. In the initial seconds due to higher spray flow the pressure increase is less steep. Nevertheless, since in the cases 2 and 3 one pressurizer PORV is modeled as rate sensitive, it opens earlier than case 1 PORVs which both open on setpoint pressure 16.2 MPa. For this reason the pressure increase in cases 2 and 3 is smaller, besides the best-estimate spray and PORVs flow. Pressurizer volume shown in Figure 14 is significantly different for case 3, because the uncertainty in the initial pressurizer level was not taken into account. Figure 15 shows the RCS average temperature and its measured signal. It may be seen that temperature increases until reactor trip. Later is the reactor trip, higher it is. The RCS average temperature is calculated from the hot and cold leg temperature, shown in Figures 16 and 17, respectively. Before the reactor trip, the differences are negligible. After the reactor trip the differences are due to different trip times and persist until hot and cold leg temperatures approach to each other. In Figure 18 is shown the pressurizer relief valves flow. It was already mentioned that rate sensitive valve open first in cases 2 and 3. The spike in cases 2 and 3 indicates opening of the second PORV on setpoint 16.2 MPa. In the case 1 both PORVs open at the same time, however their total flow is reduced. In case 1 the spike indicates the opening of the pressurizer safety valves. Steam generator no. 1 pressure is shown in Figure 19. It may be seen that the shape of cold leg temperature follows the steam generator pressure shape, which indicates that heat transfer rate to steam generators is reduced. Due to increasing pressure the steam generator safety valves open as can be seen from Figure 20. There are five safety valves per steam generator. One may see that after 25 s the valves start to close. It is clearly seen when the last two valves close. At maximum pressure four out of five steam generator safety valves were open. In Figure 21 is shown the reactor coolant system flow. It may be seen that in cases 1 and 2 the initial flow is lower than in case 3, because minimum measured flow was assumed. As the density started to decrease with increasing RCS temperature, and volumetric flow is constant, the mass flow started to decrease too. After the reactor trip the RCS mass flow started to increase. Figure 22 shows the equilibrium quality at the hottest axial location of the hot rod in the core. Increasing quality decreases the CHFR value. The CHFR trend is shown in Figure 23. It may be seen that in the period with high pressure, the CHF is set to zero and therefore CHFR is not calculated. Finally, the measured delta T and calculated OTΔT shown in Figure 24 are used for tripping the reactor. The reactor trip signal is generated when the measured delta T value reaches the calculated setpoint for OTΔT. The measured delta T does not change much with changing the initial and boundary condition, while calculated OTΔT setpoint is influenced.

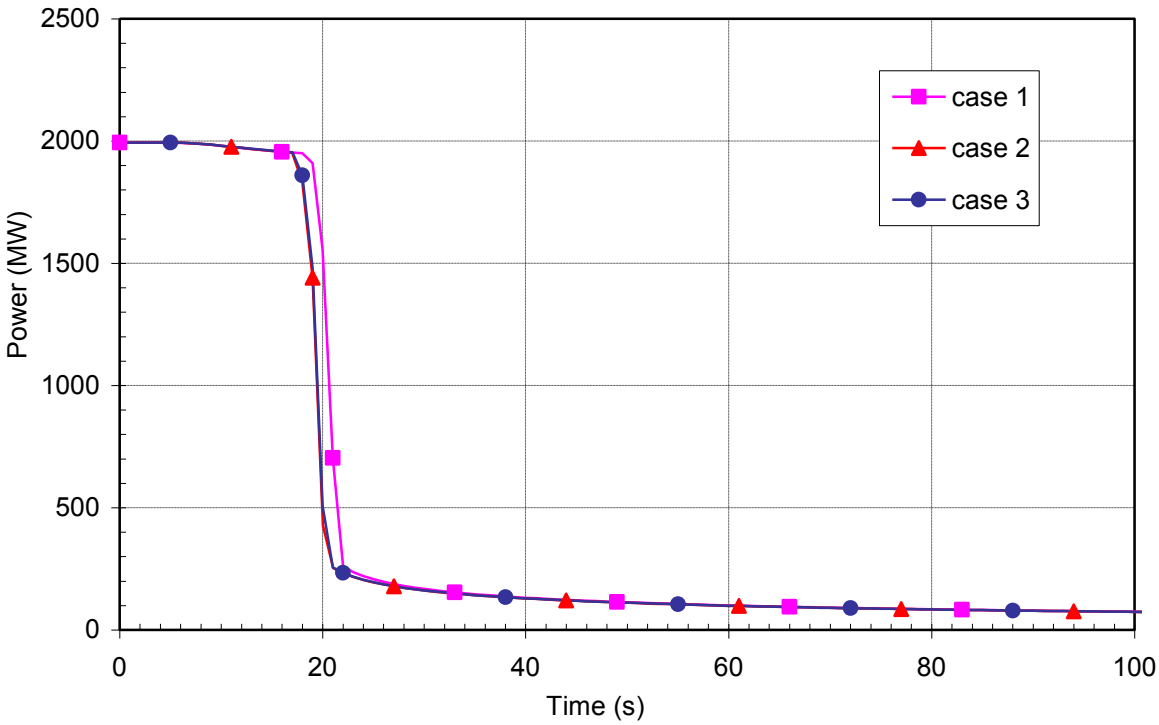

Figure 12 Reactor power – influence of I&B conditions

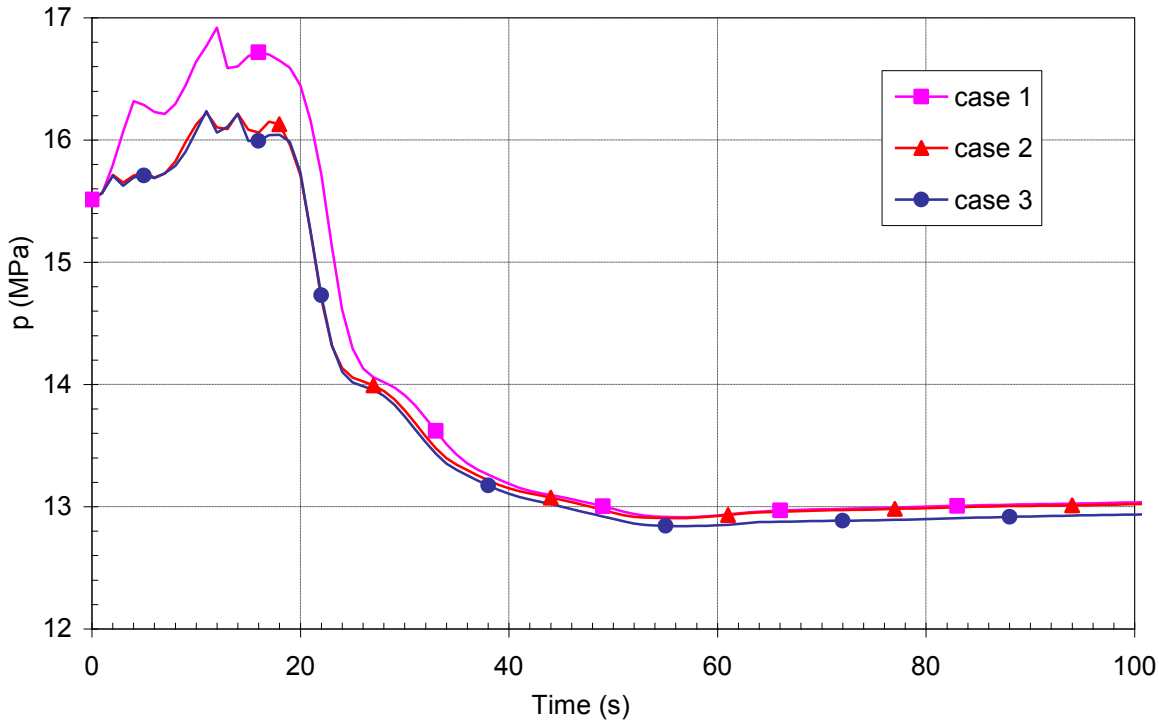

Figure 13 Pressurizer pressure - influence of I&B conditions

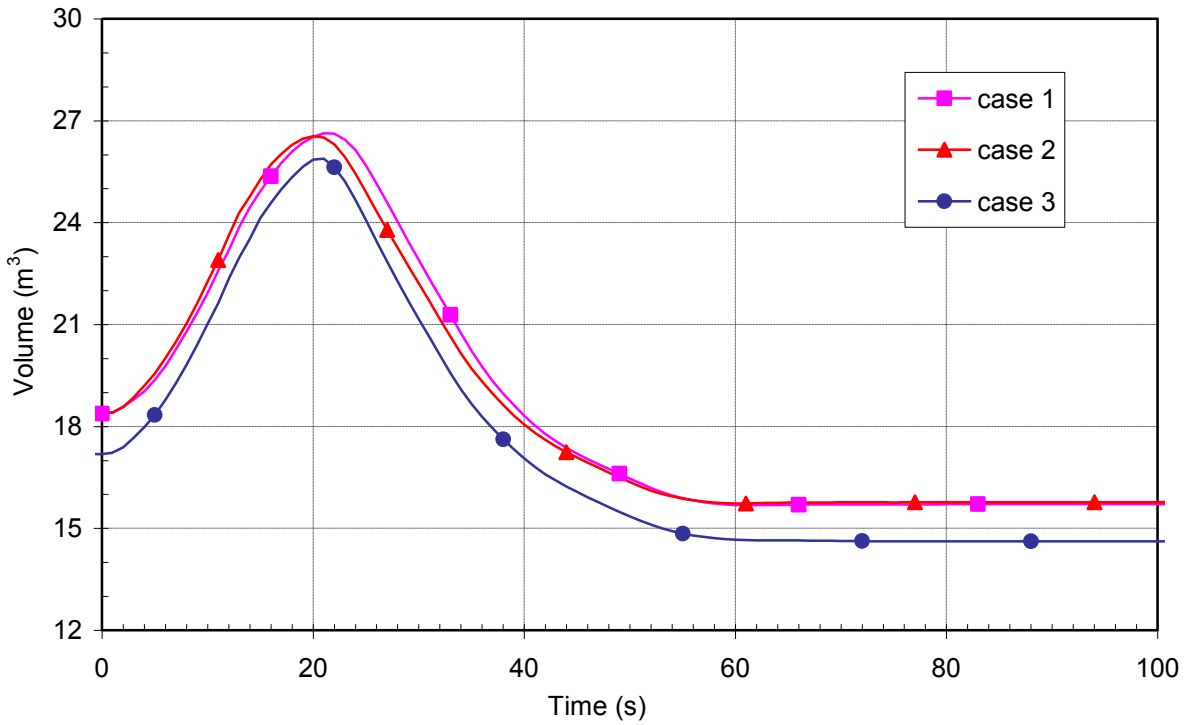

Figure 14 Pressurizer volume - influence of I&B conditions

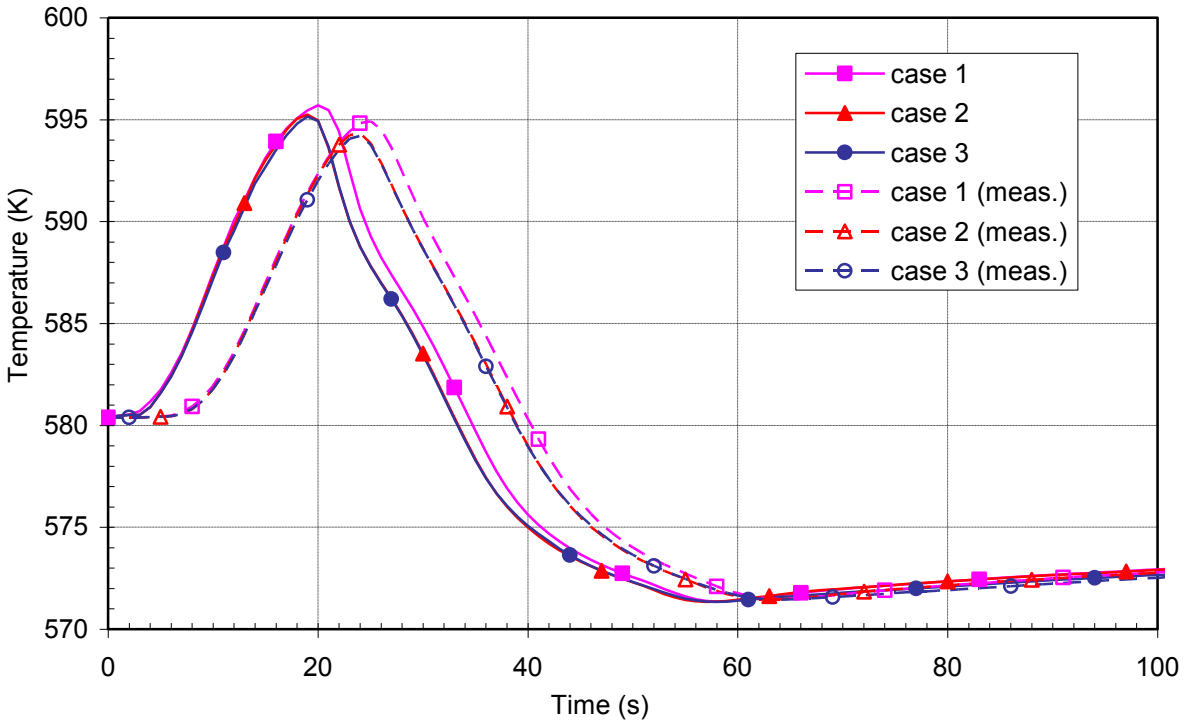

Figure 15 RCS average temperature and measured RCS average temperature - influence of I&B conditions

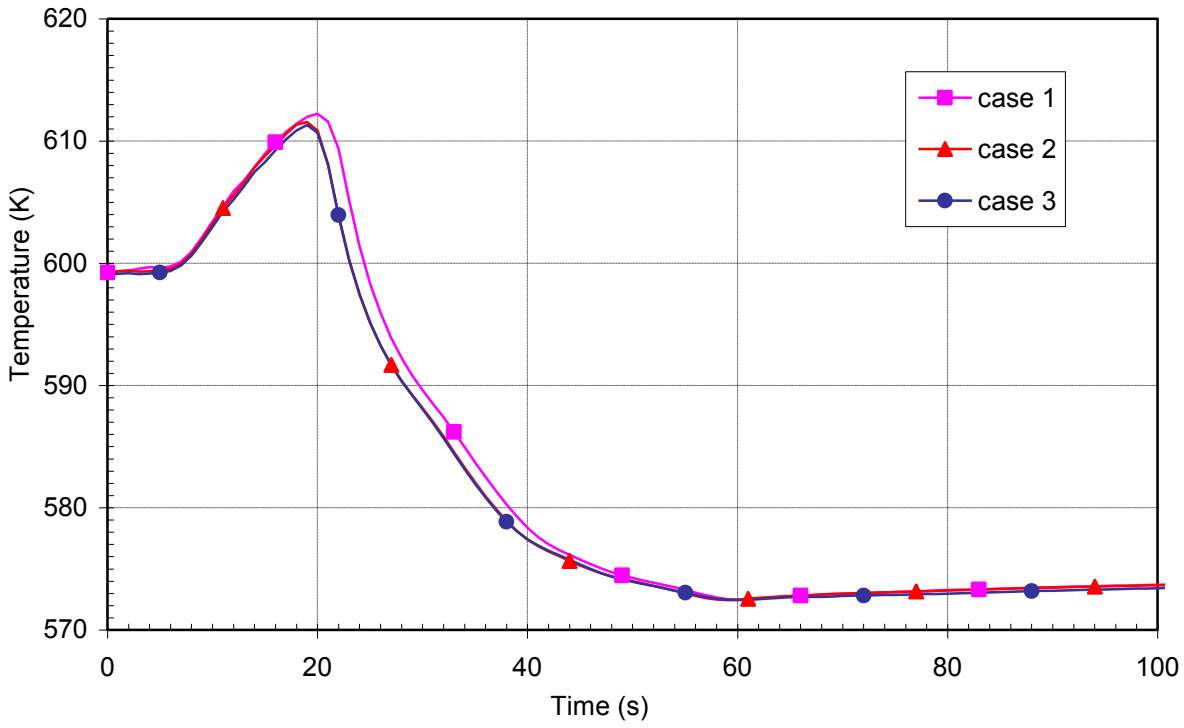

Figure 16 Hot leg no. 1 temperature - influence of I&B conditions

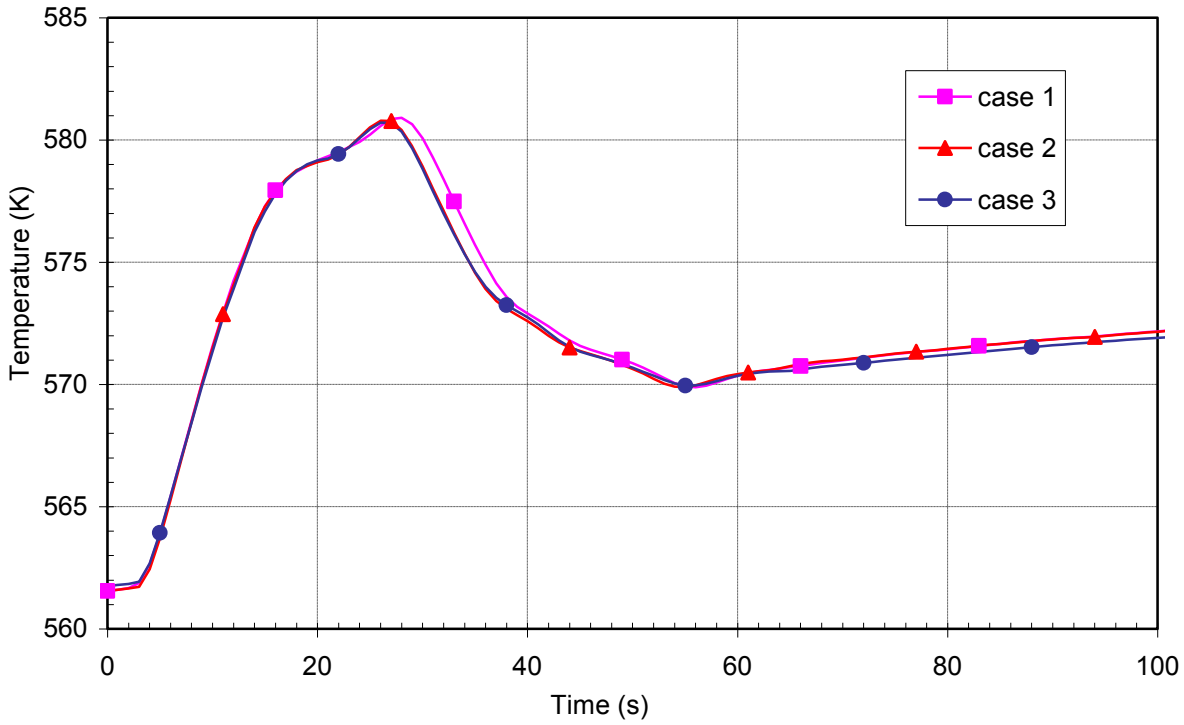

Figure 17 Cold leg no. 1 temperature - influence of I&B conditions

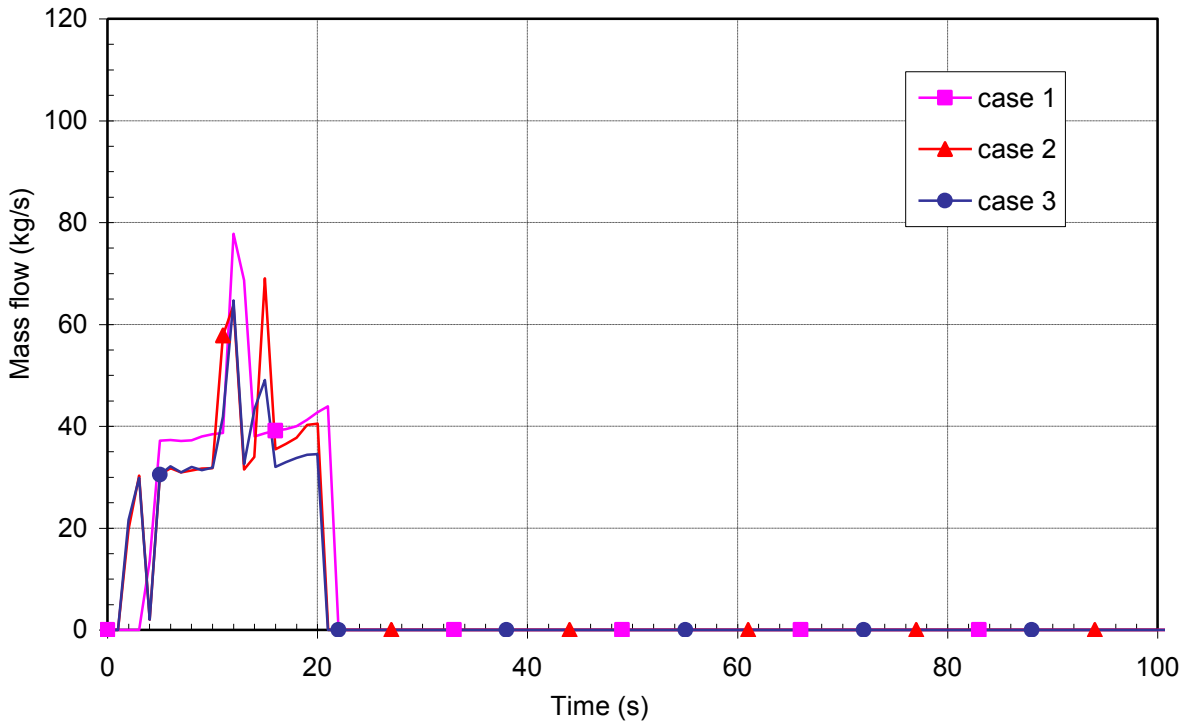

Figure 18 Pressurizer relief valves flow - influence of I&B conditions

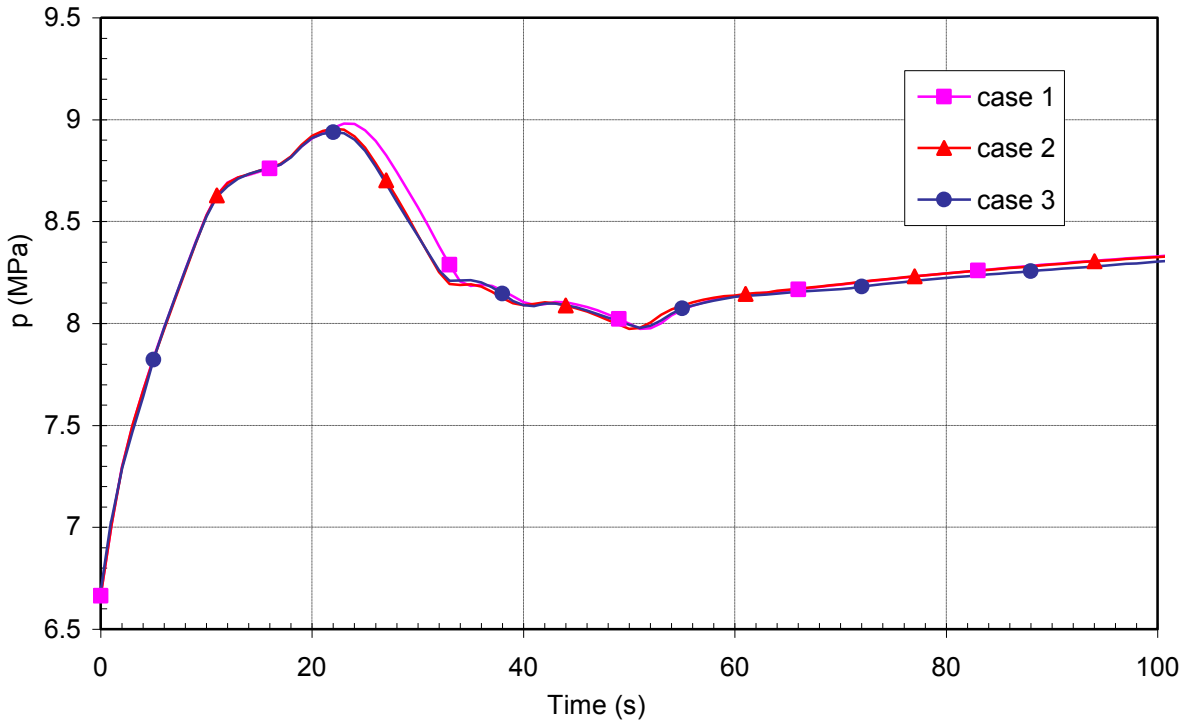

Figure 19 Steam generator no. 1 pressure - influence of I&B conditions

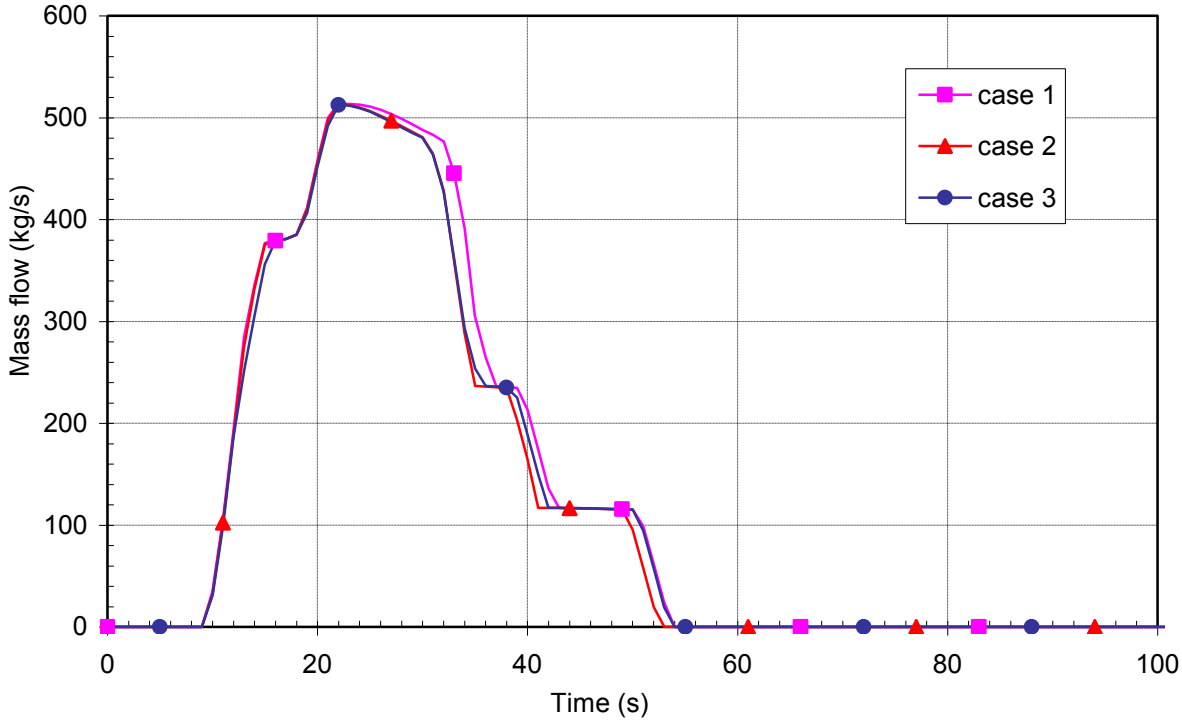

Figure 20 Steam generator no. 1 relief valves mass flow - influence of I&B conditions

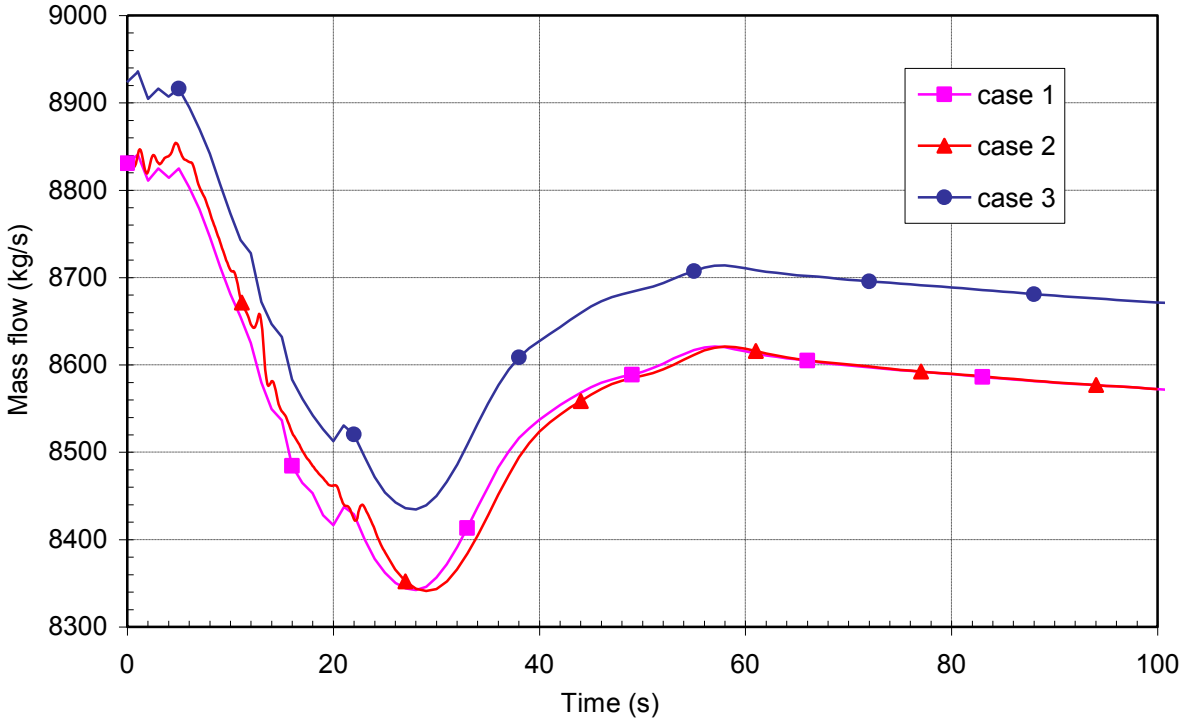

Figure 21 Mass flow through hottest axial location in the core - influence of I&B conditions

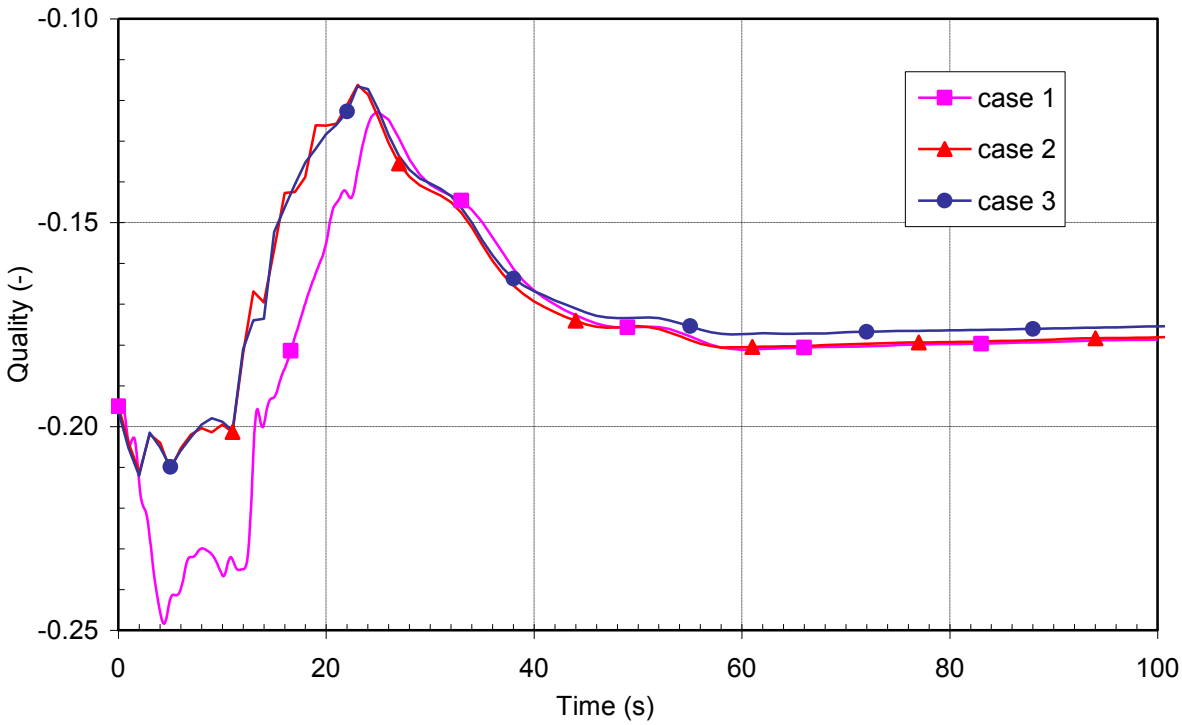

Figure 22 Equilibrium quality at the hottest axial location in the core - influence of I&B conditions

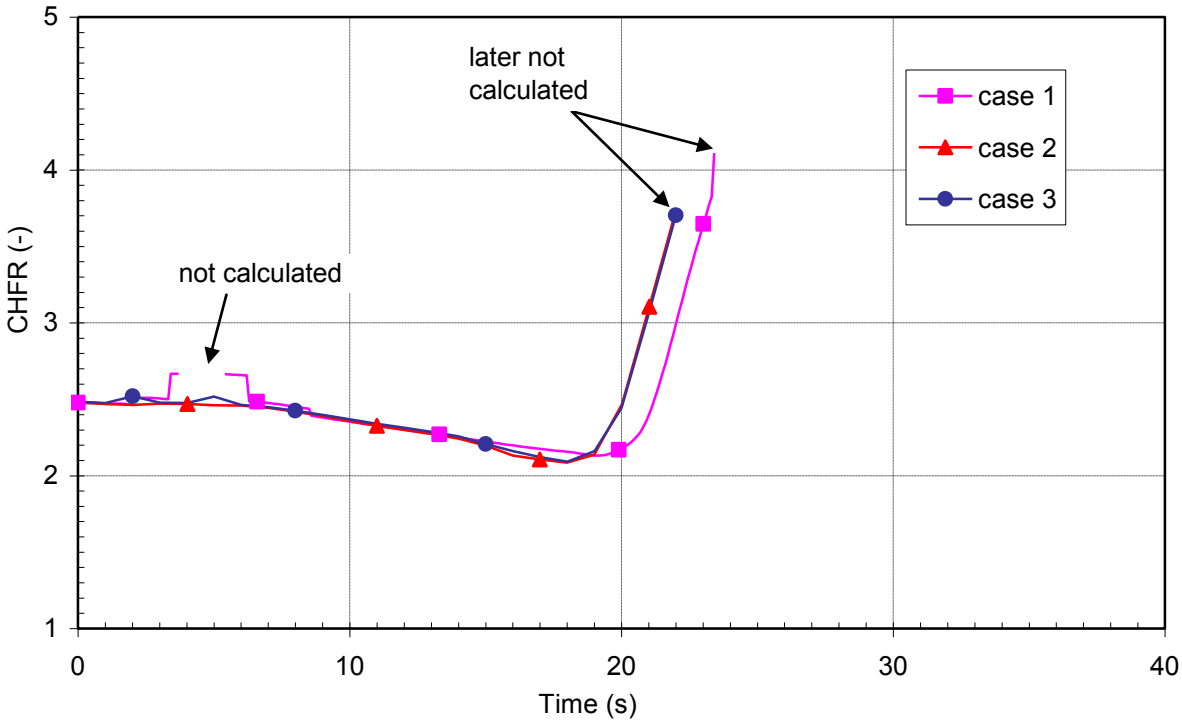

Figure 23 Critical heat flux ratio - influence of I&B conditions

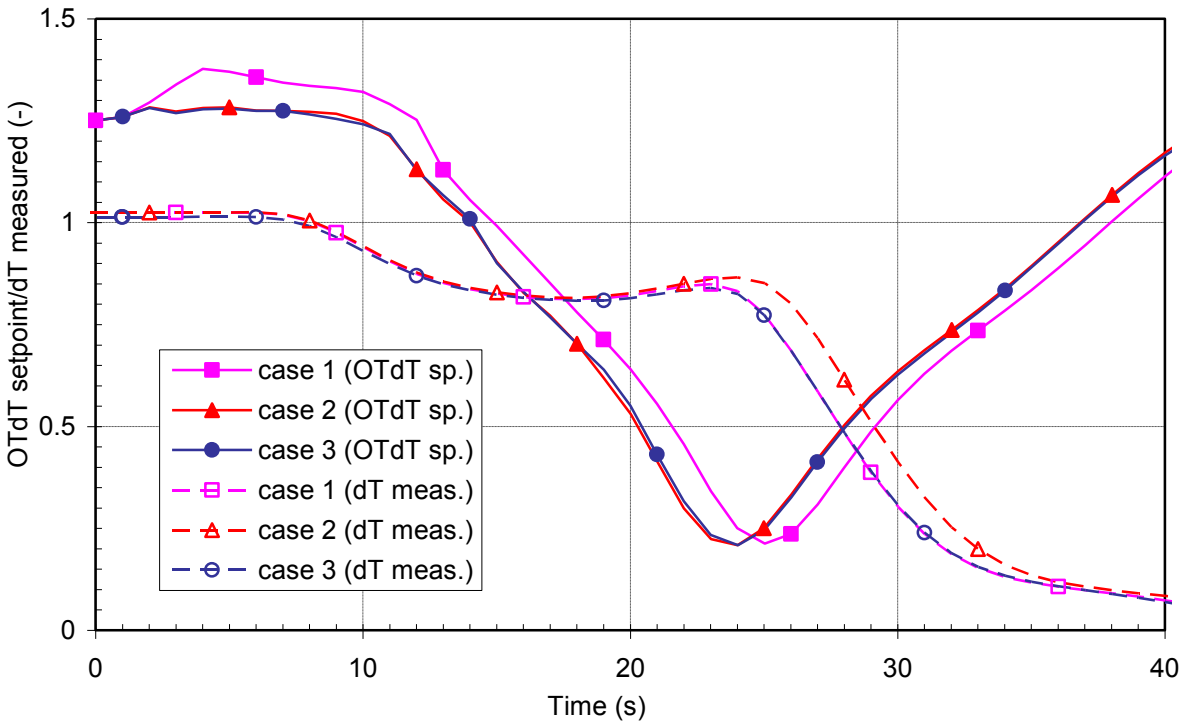

Figure 24 Overtemperature ΔT setpoint calculation and measured delta T - influence of I&B conditions

5.2.2 Variation of Measurement Delay Time for Case 1

In Figures 25 through 33 are shown the most important variables used for OTΔT setpoint and CHFR calculation for different measurement delays. The measurement time delay initially influences the reactor trip time on OTΔT signal, which in turn influences the other variables, used for CHFR calculation. After the reactor trip the pressurizer pressure (see Figure 25) drops significantly. Similar is the situation for RCS average temperature shown in Figure 26. Important is the fact that the larger the measurement delay is, the larger the temperature increase is. With increasing RCS average temperature the mass flow is decreasing due to lower density of the coolant as can be seen from Figure 27. Also it can be seen that the mass flow decreases with increasing measurement delay. The equilibrium quality (see Figure 28) initially decreases when the pressure is increasing and later increases due to dropping pressure. The CHFR shown in Figure 29 initially increases due to pressure increase. After pressure drop it started to decrease almost linearly. This means the later is the trip, the smaller is the minimum CHFR. Finally, the temperature and pressure terms for OTΔT setpoint calculation are shown in Figures 30 and 31, respectively. The equation for OTΔT setpoints has a constant 1.25 from which the temperature term K2 is subtracted and the pressure term K3 is added. This means that in the initial period the temperature decreases the setpoint while the pressure increases it. After 10 seconds the temperature term K2 becomes dominating. From Figure 32 it can be seen how the OTΔT setpoint decrease is delayed proportionally to the measurement delay time. Finally, also measured delta T is influenced by measurement delay. Nevertheless, at the time of reactor trip the measurement delay is no more influential. The results of sensitivity analysis showed that when the temperature measurement delay is rather small (e.g. ± 2 seconds with respect to base case), also the reactor trip on OTΔT signal is similarly delayed. The delays impact the curves of important plant variables in such a way that the trend direction is continued for delay time difference and after the reactor trip the curves are time shifted, when compared to each other. As CHFR calculation depends on pressure, mass flux and equilibrium quality, the same is true for CHFR as for these parameters.

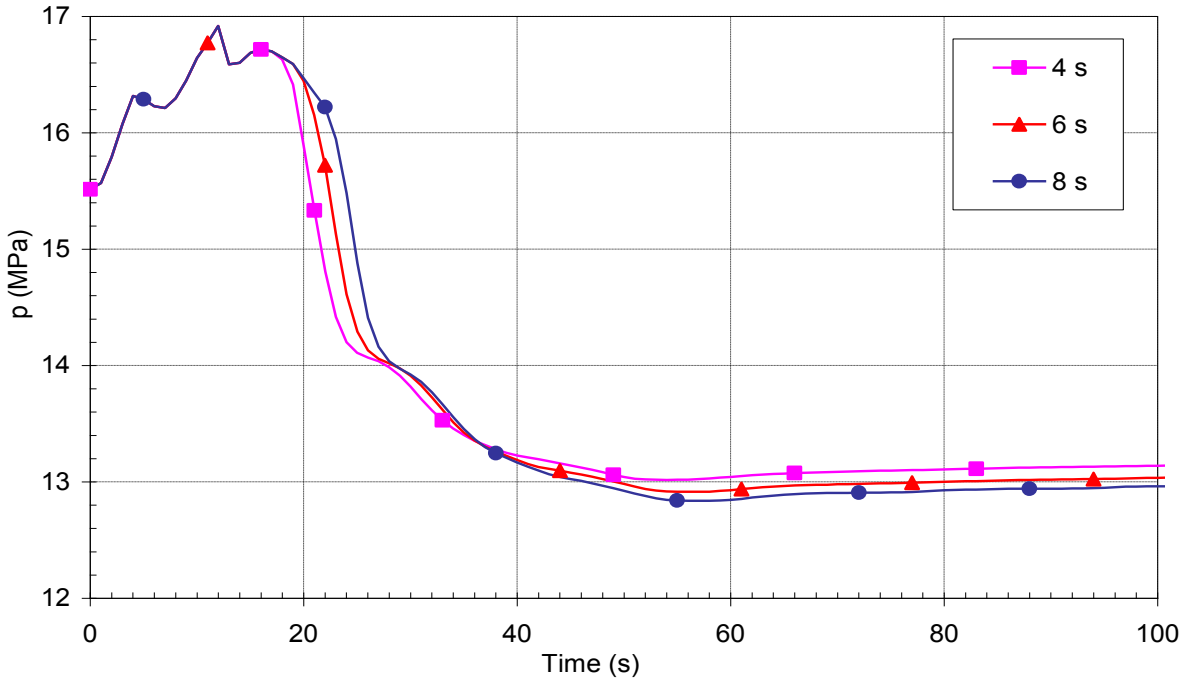

Figure 25 Pressurizer pressure - influence of measurement delay for case 1

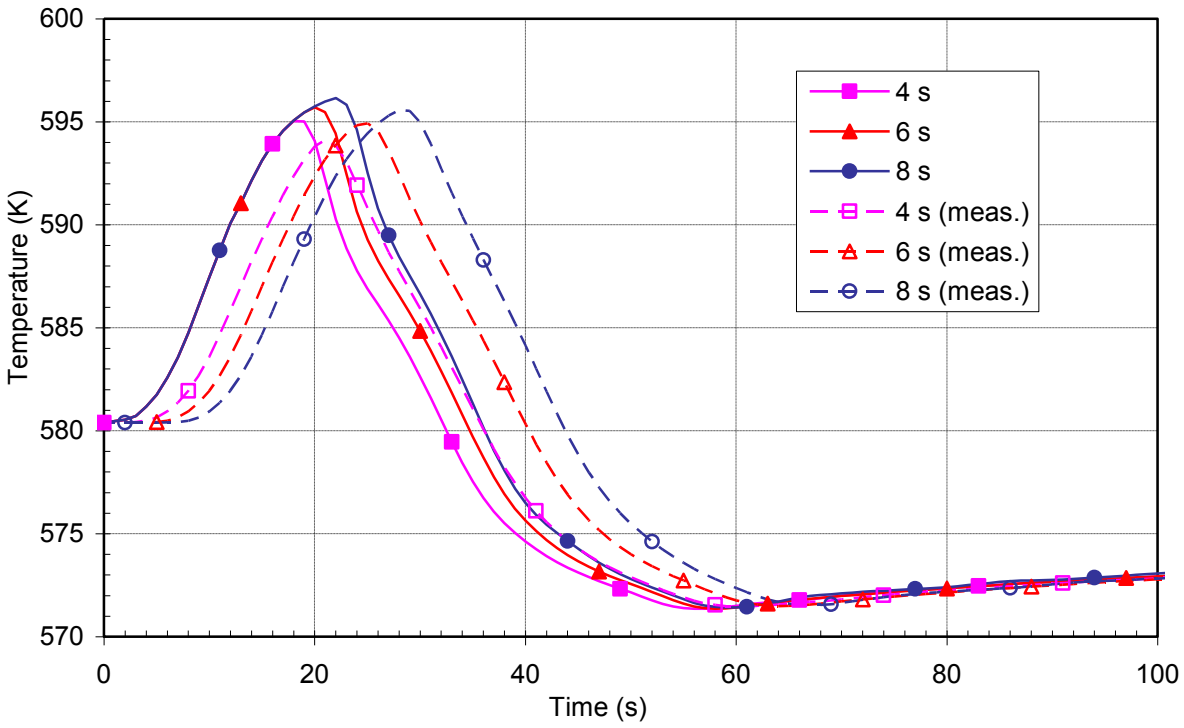

Figure 26 RCS average temperature and measured RCS average temperature - influence of measurement delay for case 1

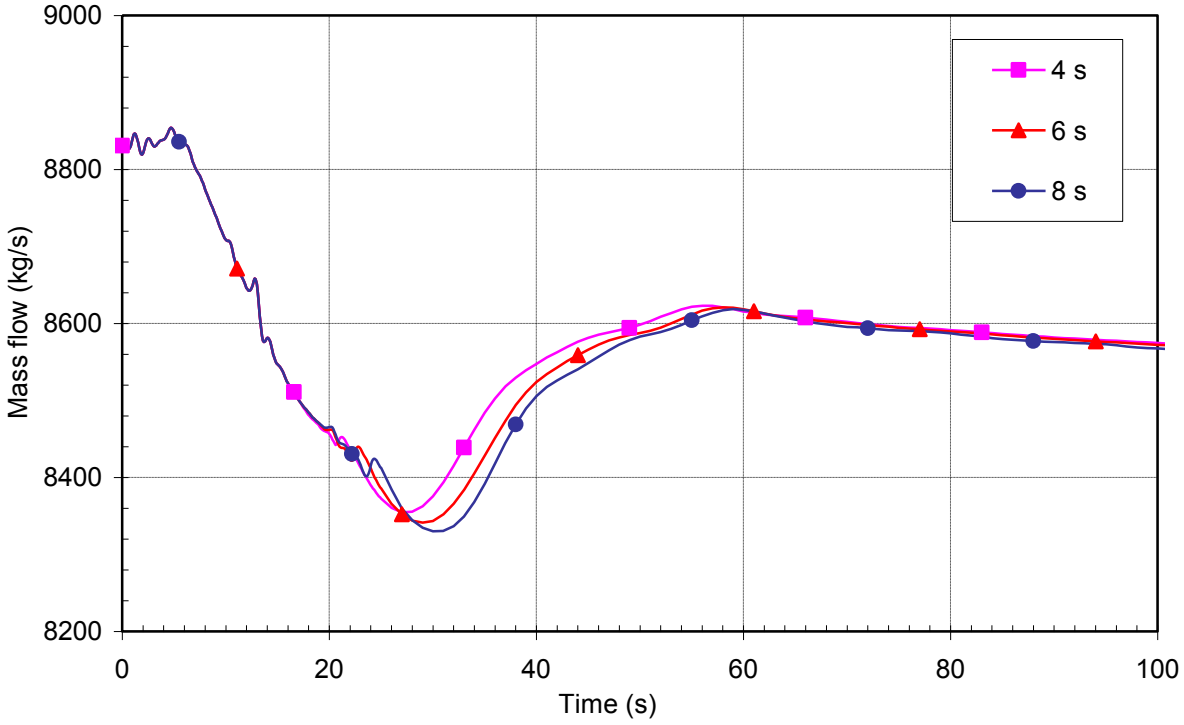

Figure 27 Mass flow through hottest axial location in the core - influence of measurement delay for case 1

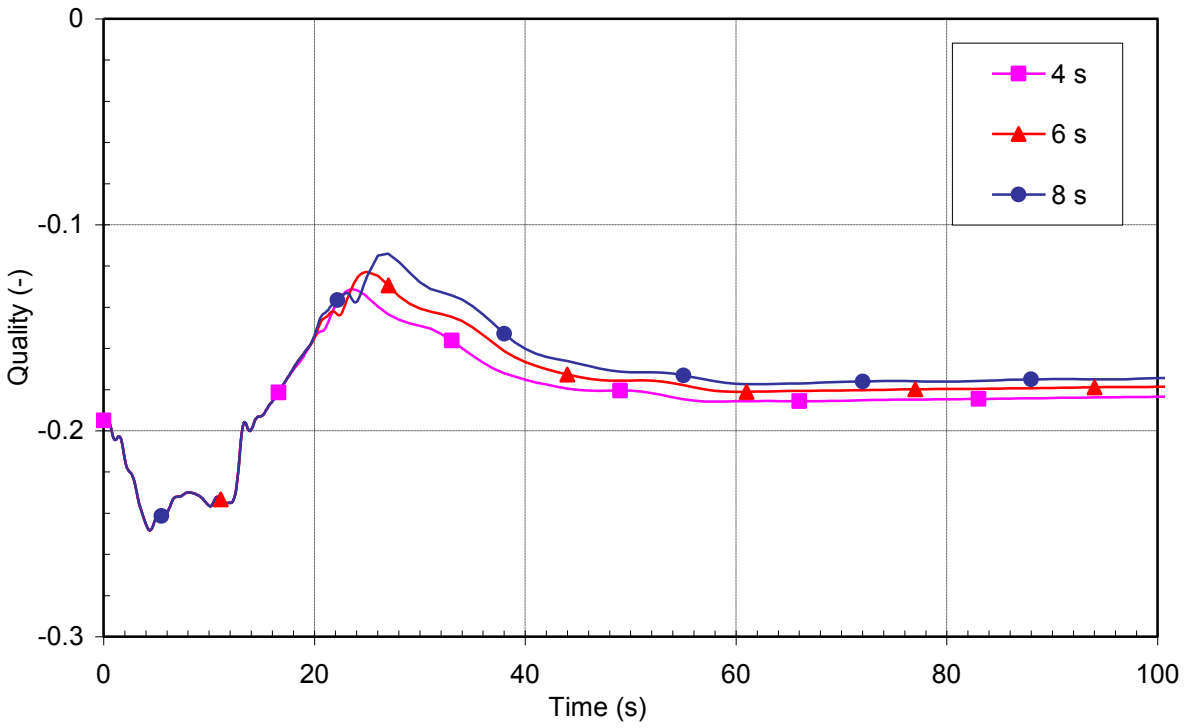

Figure 28 Equilibrium quality at the hottest axial location in the core - influence of measurement delay for case 1

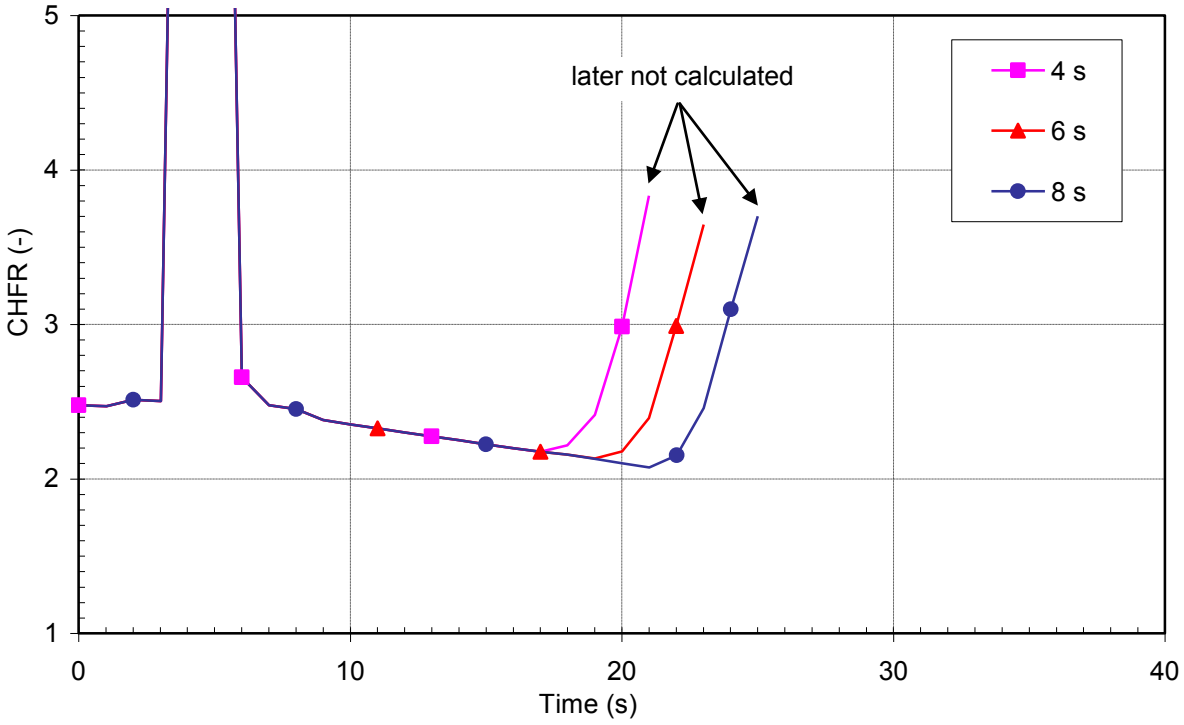

Figure 29 Critical heat flux ratio - influence of measurement delay for case 1

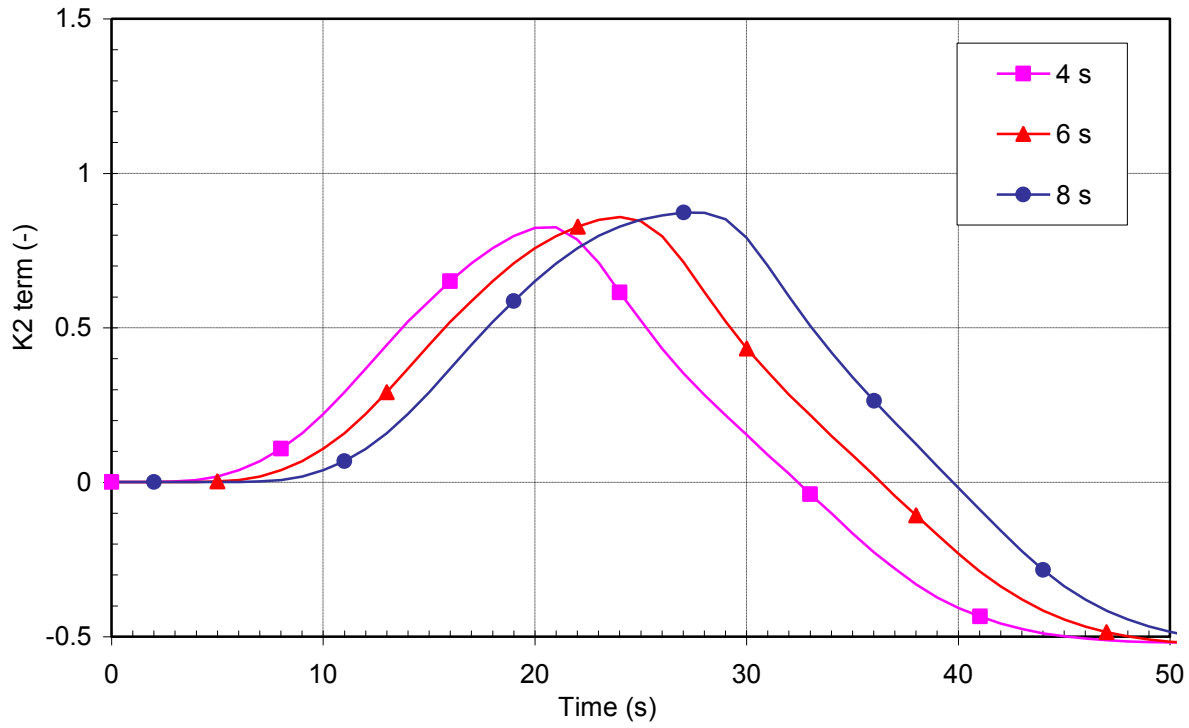

Figure 30 K2 temperature term calculation - influence of measurement delay for case 1

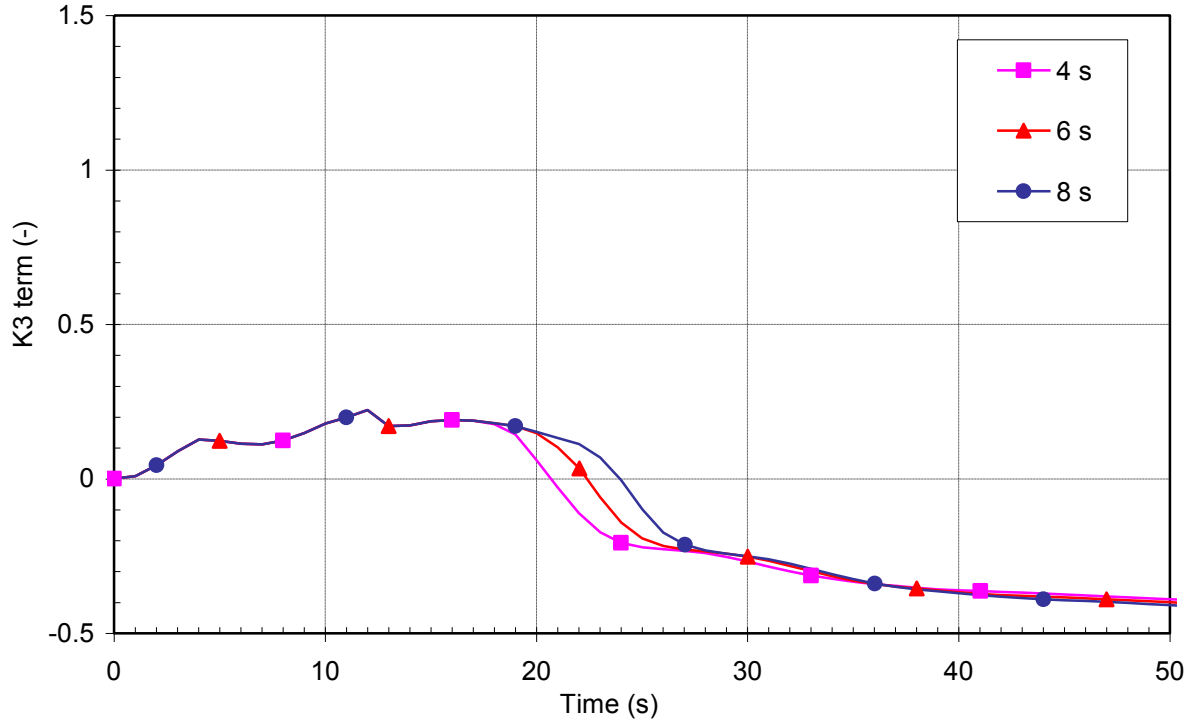

Figure 31 K3 pressure term calculation - influence of measurement delay for case 1

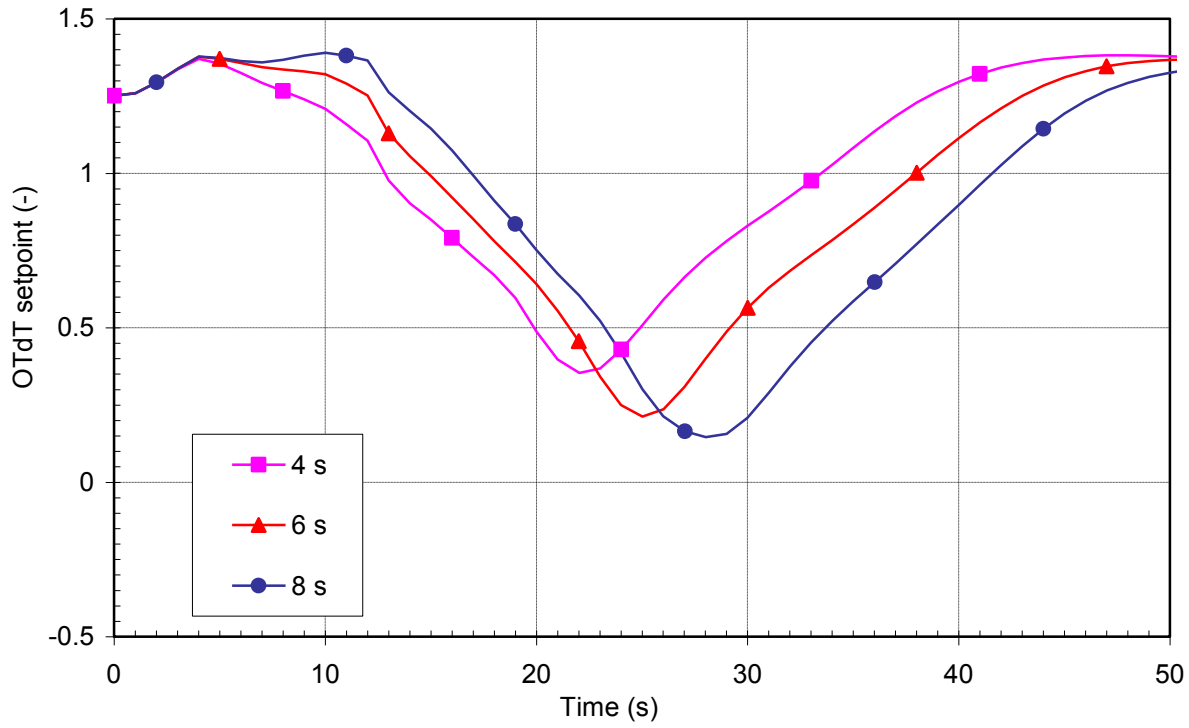

Figure 32 Overtemperature ΔT setpoint calculation - influence of measurement delay for case 1

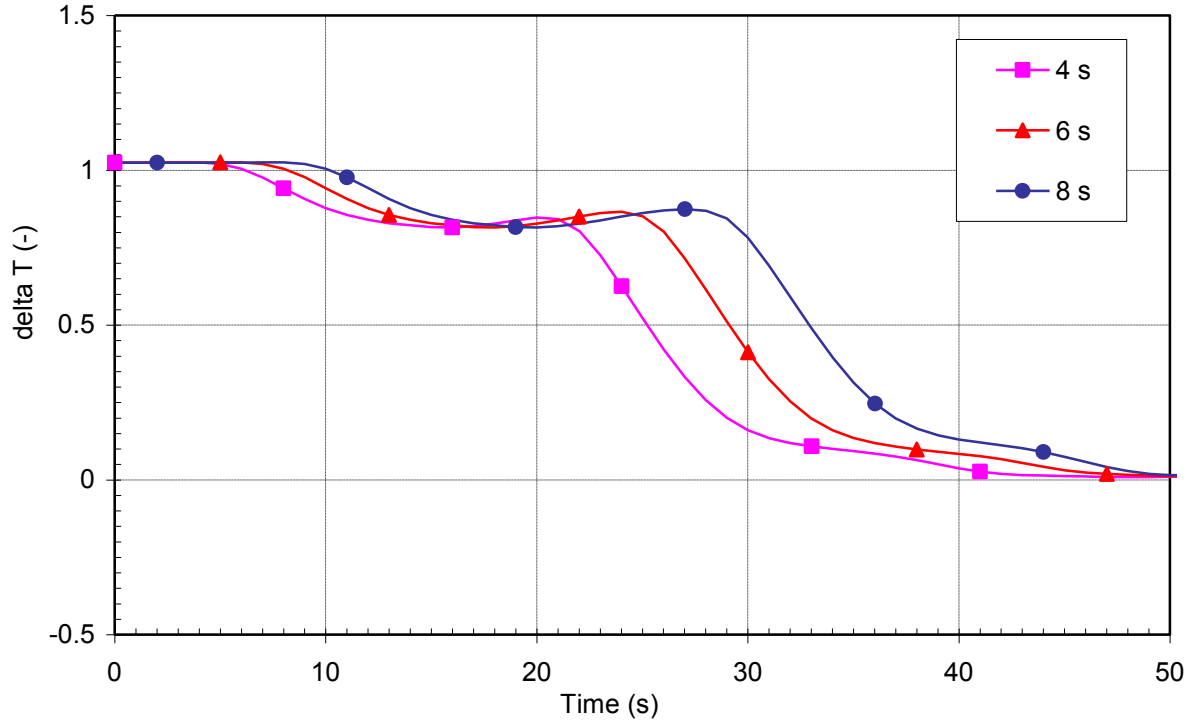

Figure 33 Measured delta T - influence of measurement delay for case 1

5.2.3 Variation of Measurement Delay Time for Case 2

Figures 34 through 42 show the case 2 calculation, in which primary side heat transfer is not compensated like in base calculation. The results show that for case 2 same can be said as for case 1. When the temperature measurement delay is rather small (e.g. ± 2 seconds with respect to base case), also the trip on OTΔT is similarly delayed.

To additionally confirm this, the delay +8 seconds with respect to base case is presented. From Figure 35 it can be seen that the measured RCS average temperature is time shifted and the peak temperature is higher when measurement delay is larger. On the other hand the mass flow decreases (see Figure 36) more, while the equilibrium quality (see Figure 37) and RCS average temperature (see Figure 36) increase with larger time delay. The results for delay +8 seconds (see Figures 38 through 42) also support the statement that the larger the measurement delay is, the later is the reactor trip on OTΔT and smaller is the minimal CHFR.

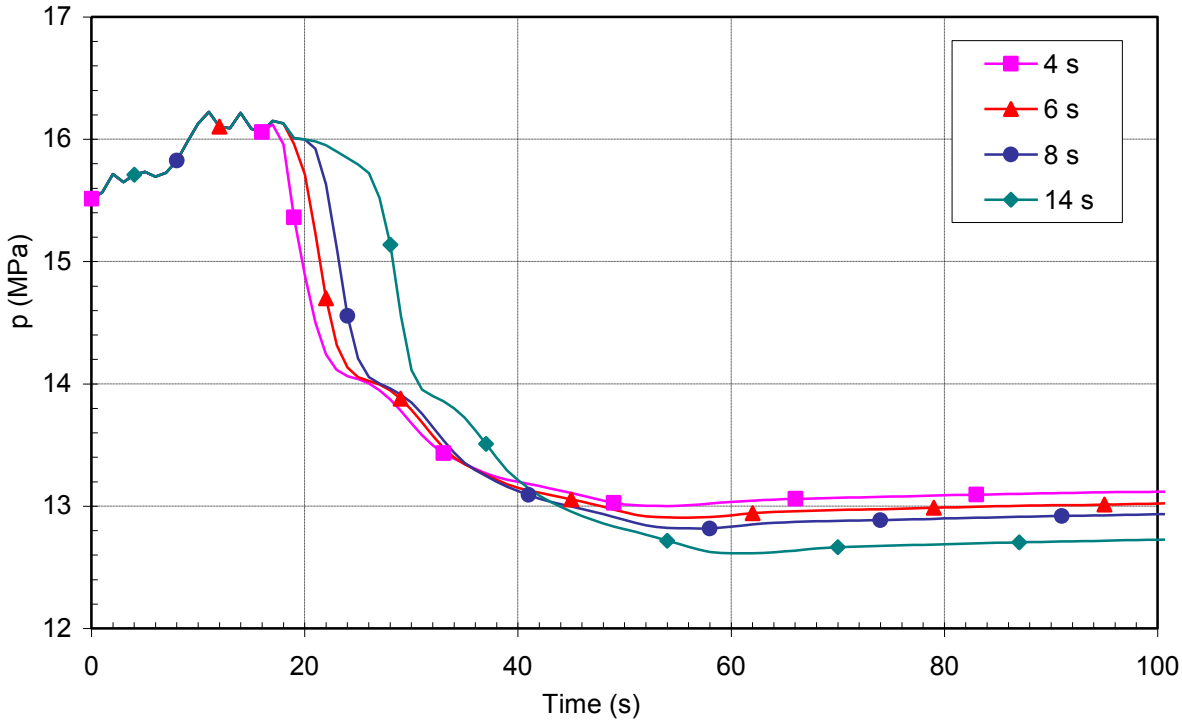

Figure 34 Pressurizer pressure - influence of measurement delay for case 2

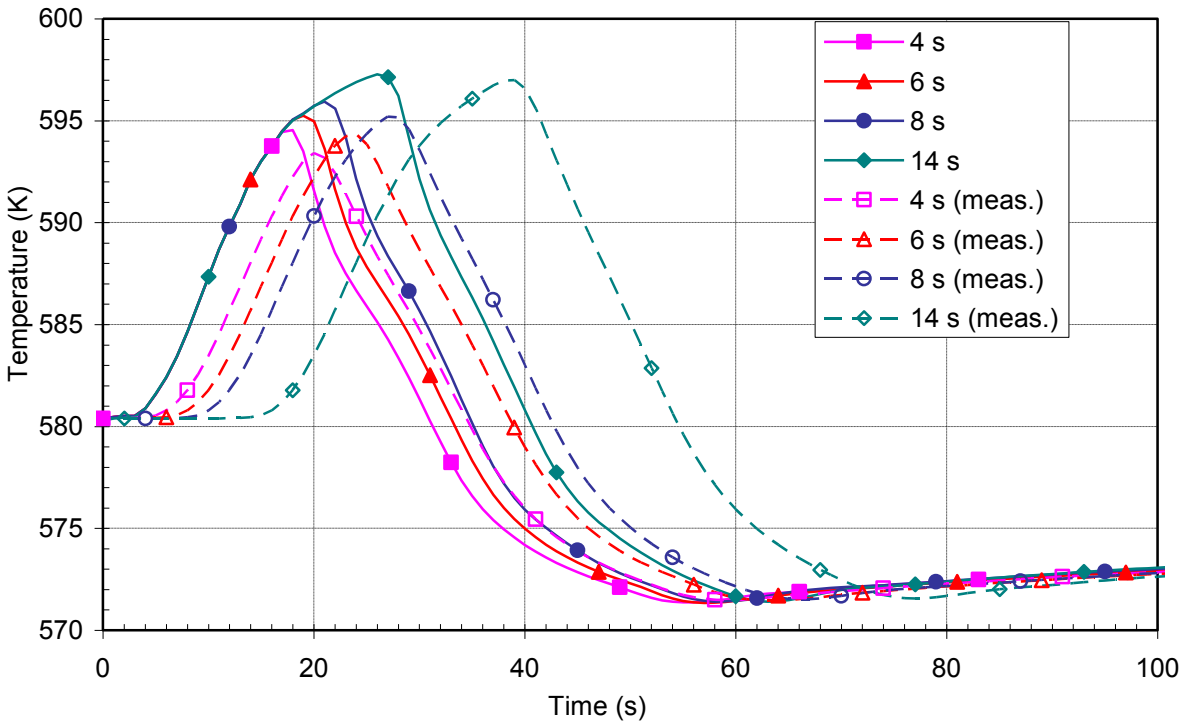

Figure 35 RCS average temperature and measured RCS average temperature - influence of measurement delay for case 2

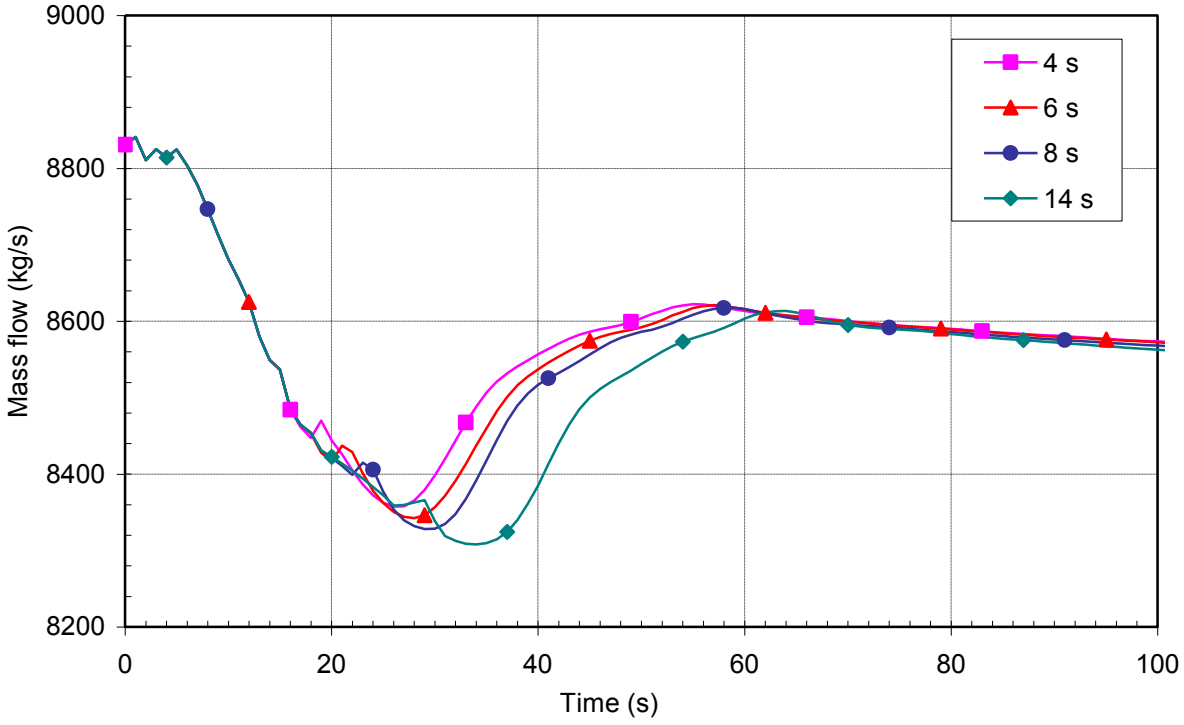

Figure 36 Mass flow through hottest axial location in the core - influence of measurement delay for case 2

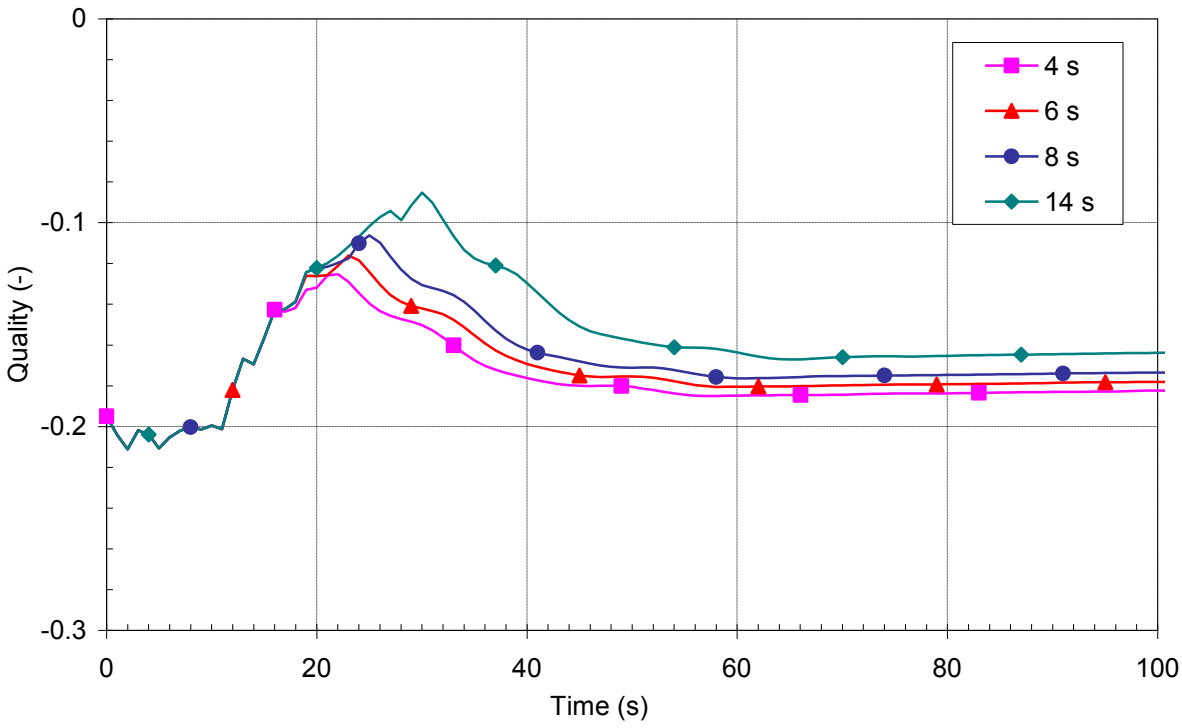

Figure 37 Equilibrium quality at the hottest axial location in the core - influence of measurement delay for case 2

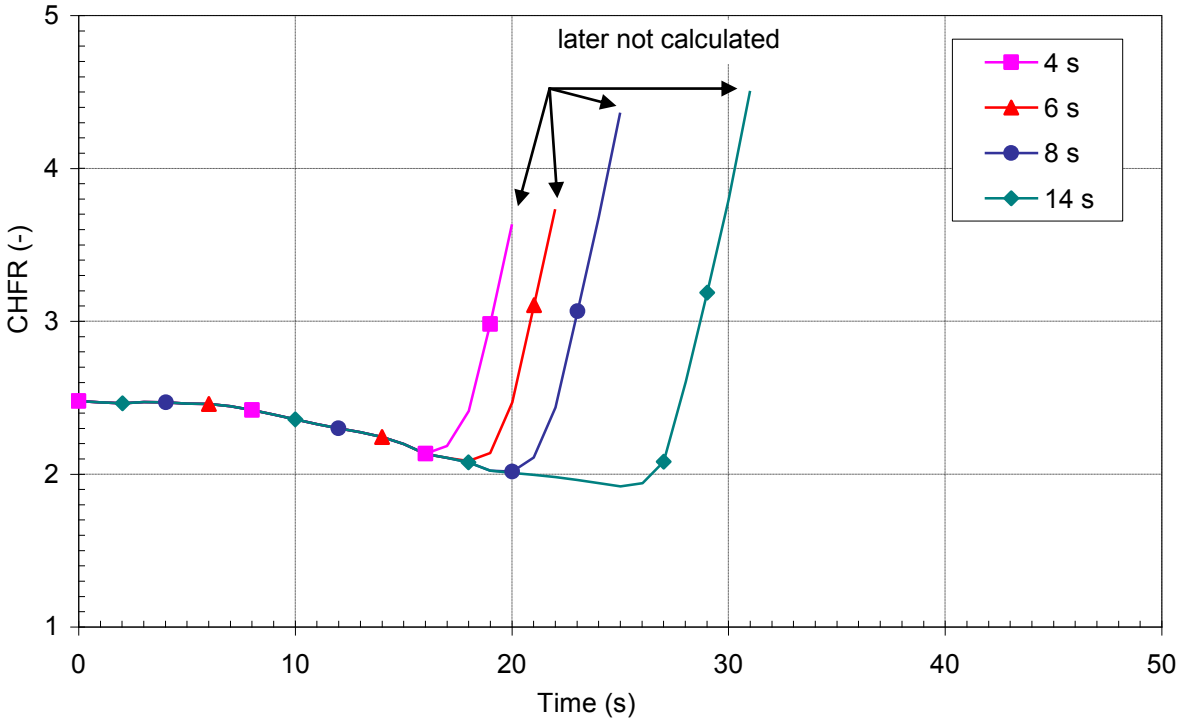

Figure 38 Critical heat flux ratio - influence of measurement delay for case 2

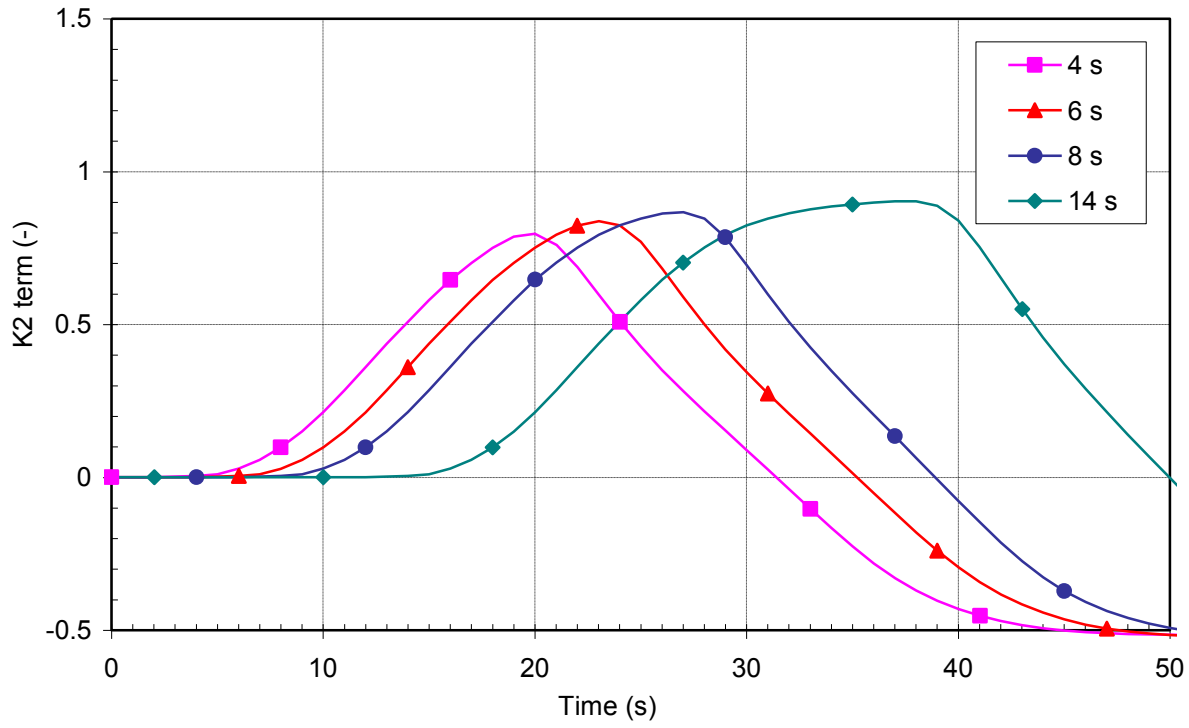

Figure 39 K2 temperature term calculation - influence of measurement delay for case 2

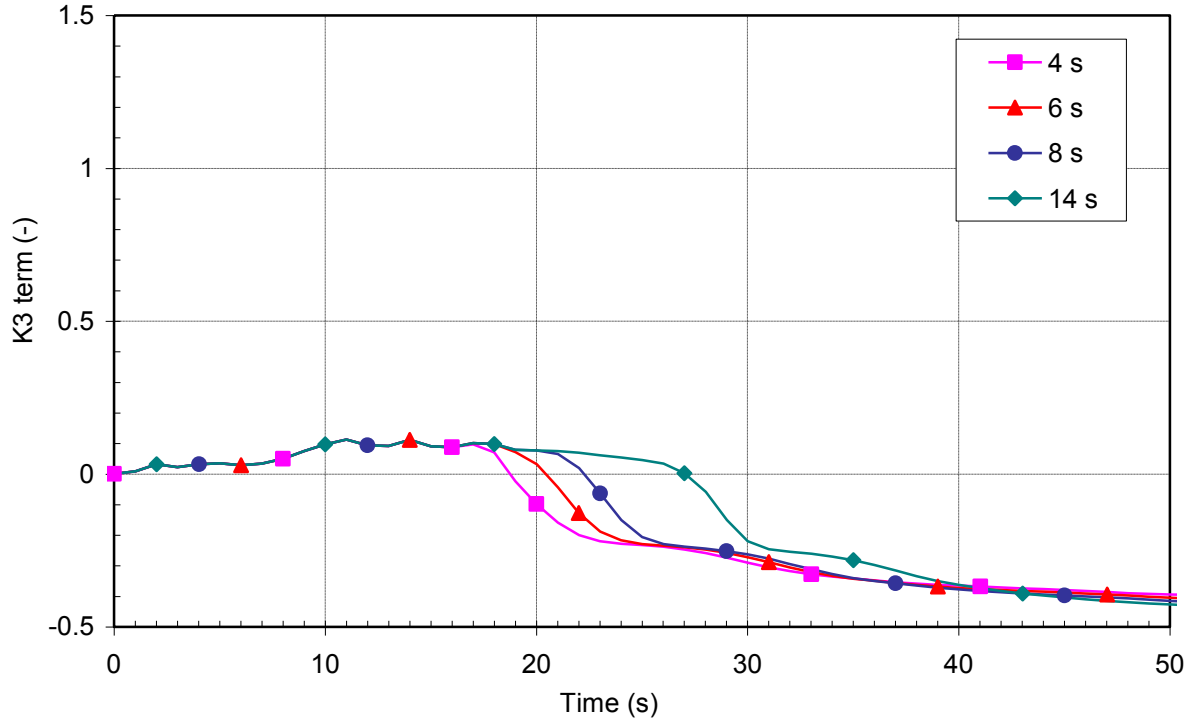

Figure 40 K3 pressure term calculation - influence of measurement delay for case 2

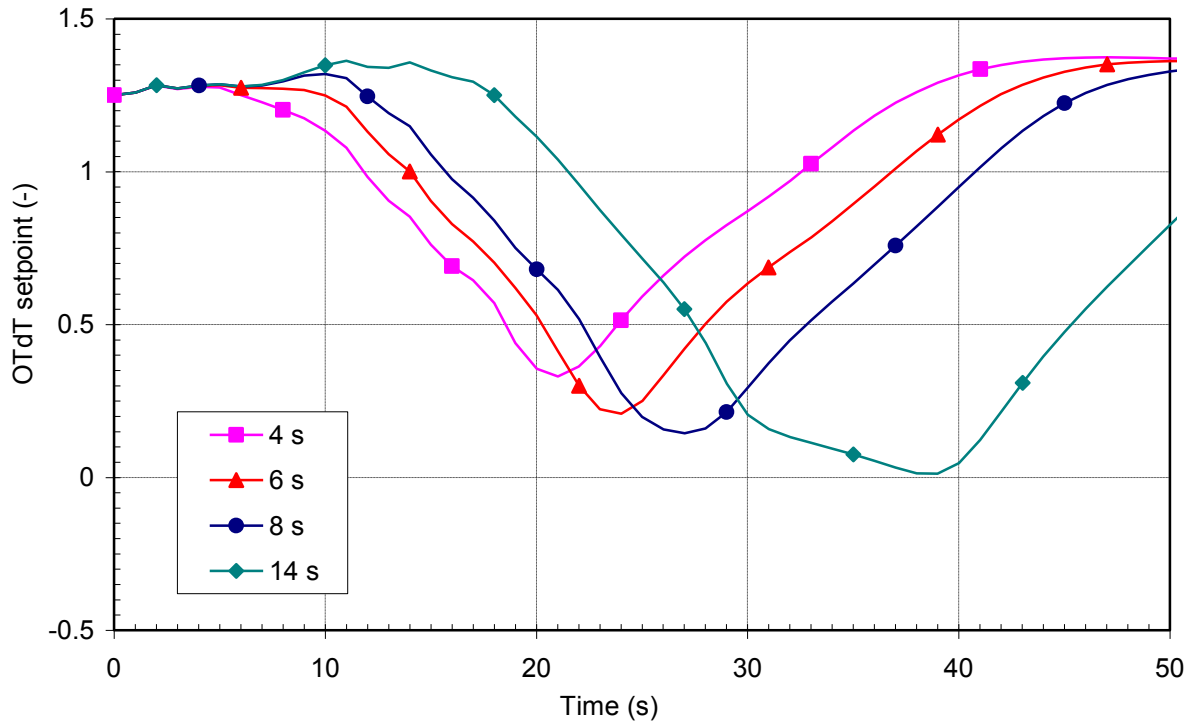

Figure 41 Overtemperature ΔT setpoint calculation - influence of measurement delay for case 2

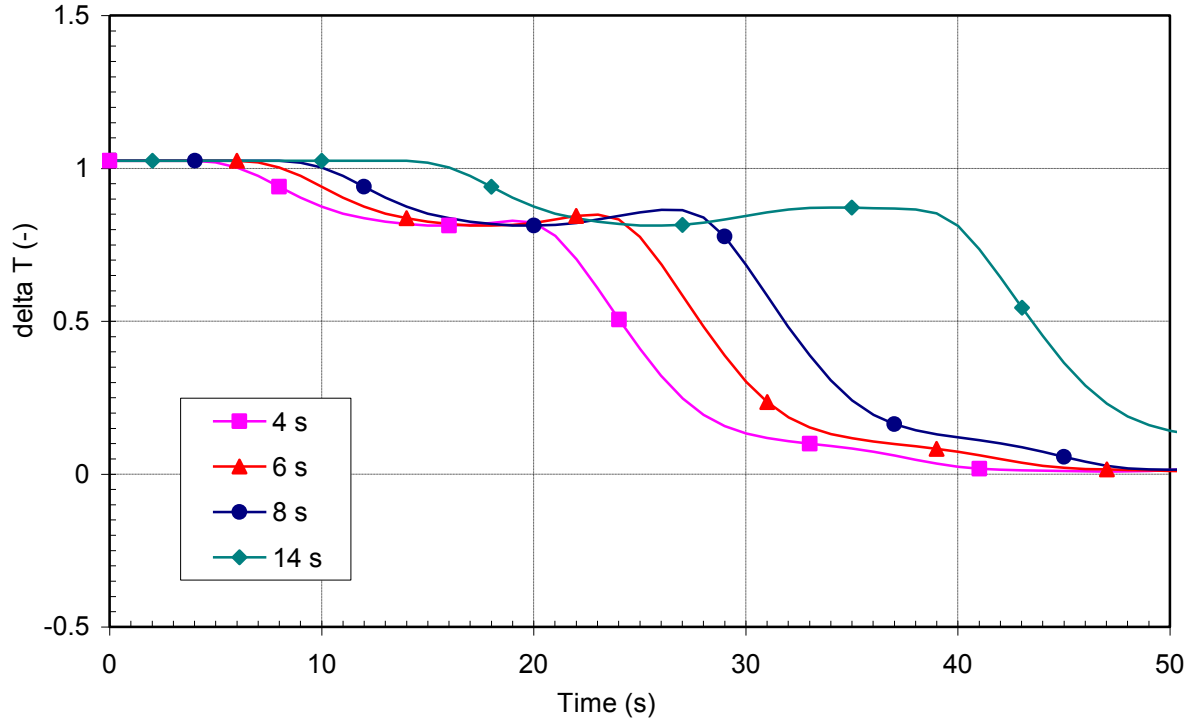

Figure 42 Measured delta T - influence of measurement delay for case 2

5.2.4 Variation of Measurement Delay Time for Case 3

Figures 43 through 51 show variation of time delay for case 3. Again it can be said that the delays impact the curves of important plant variables in such a way that the trend direction is continued for delay time difference and after the reactor trip the curves are time shifted, when compared to each other. As CHFR calculation depends on pressure, mass flux and equilibrium quality, the same is true for CHFR as for these parameters. The larger the measurement delay is, the later the reactor trip on OTΔT is and the smaller the minimal CHFR is.

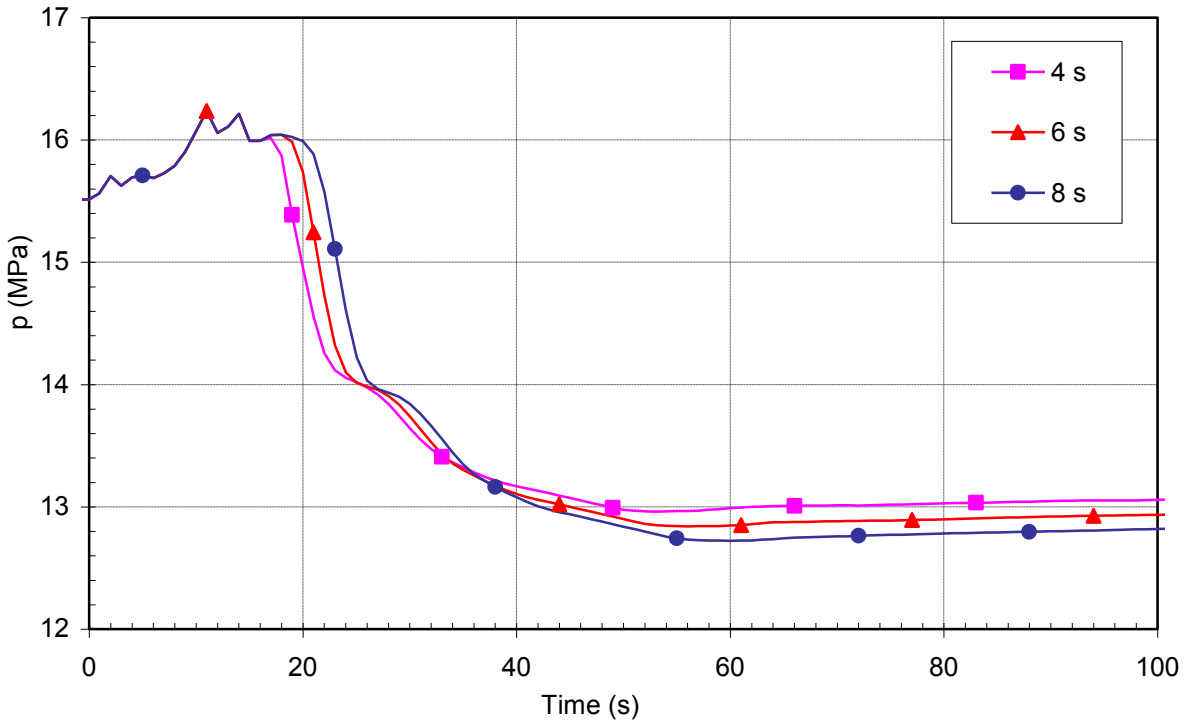

Figure 43 Pressurizer pressure - influence of measurement delay for case 3

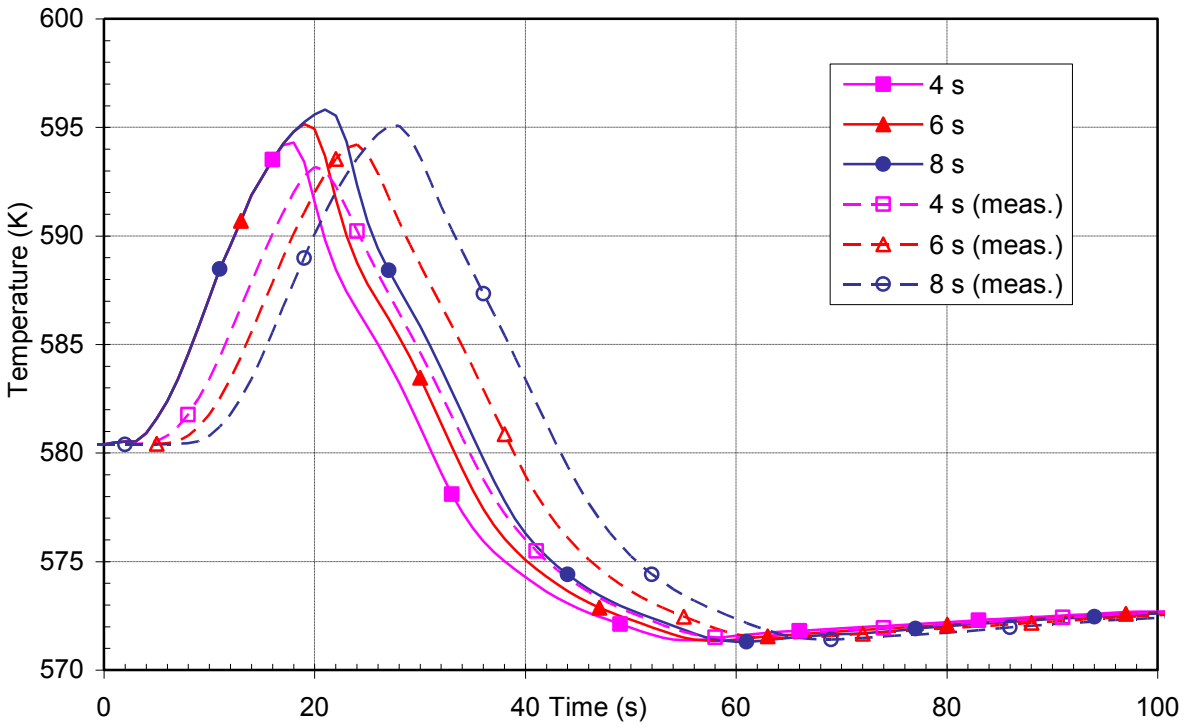

Figure 44 RCS average temperature and measured RCS average temperature - influence of measurement delay for case 3

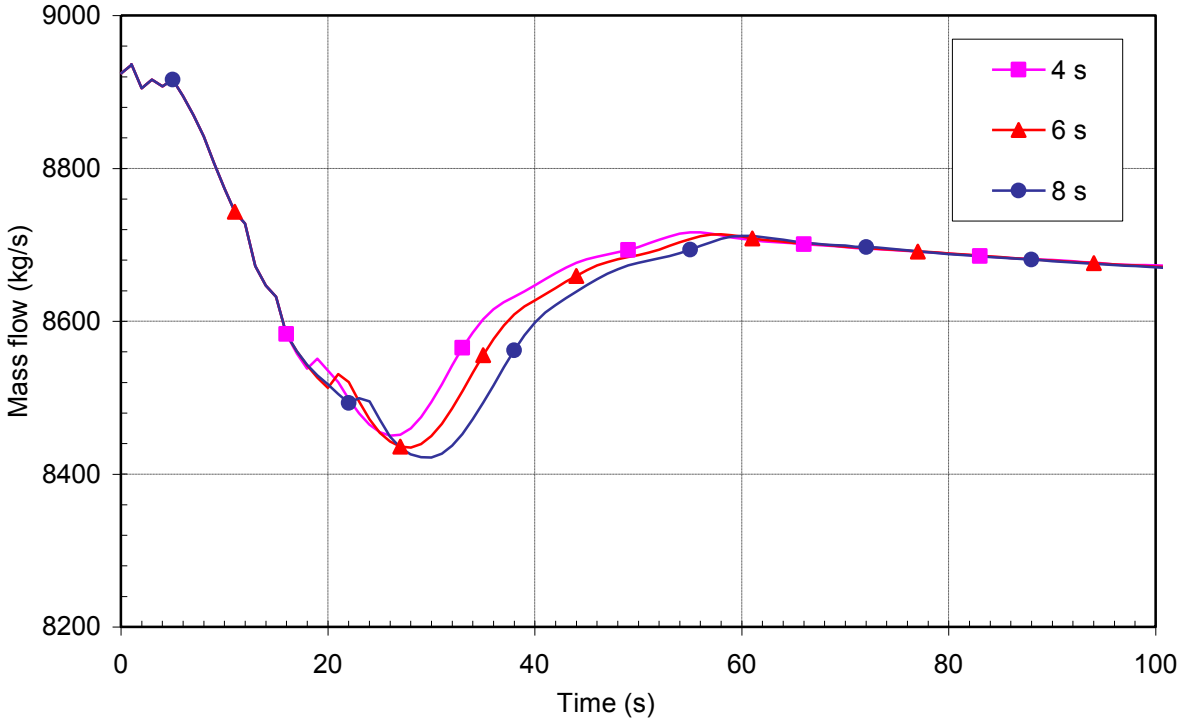

Figure 45 Mass flow through hottest axial location in the core - influence of measurement delay for case 3

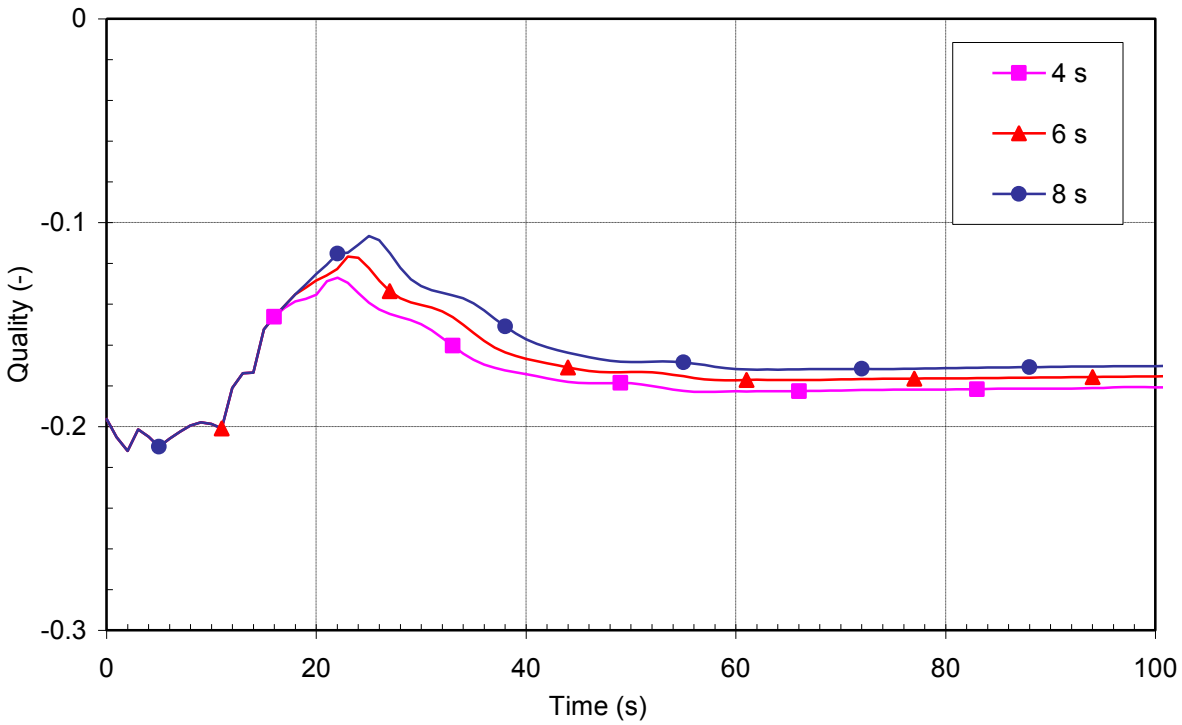

Figure 46 Equilibrium quality at the hottest axial location in the core - influence of measurement delay for case 3

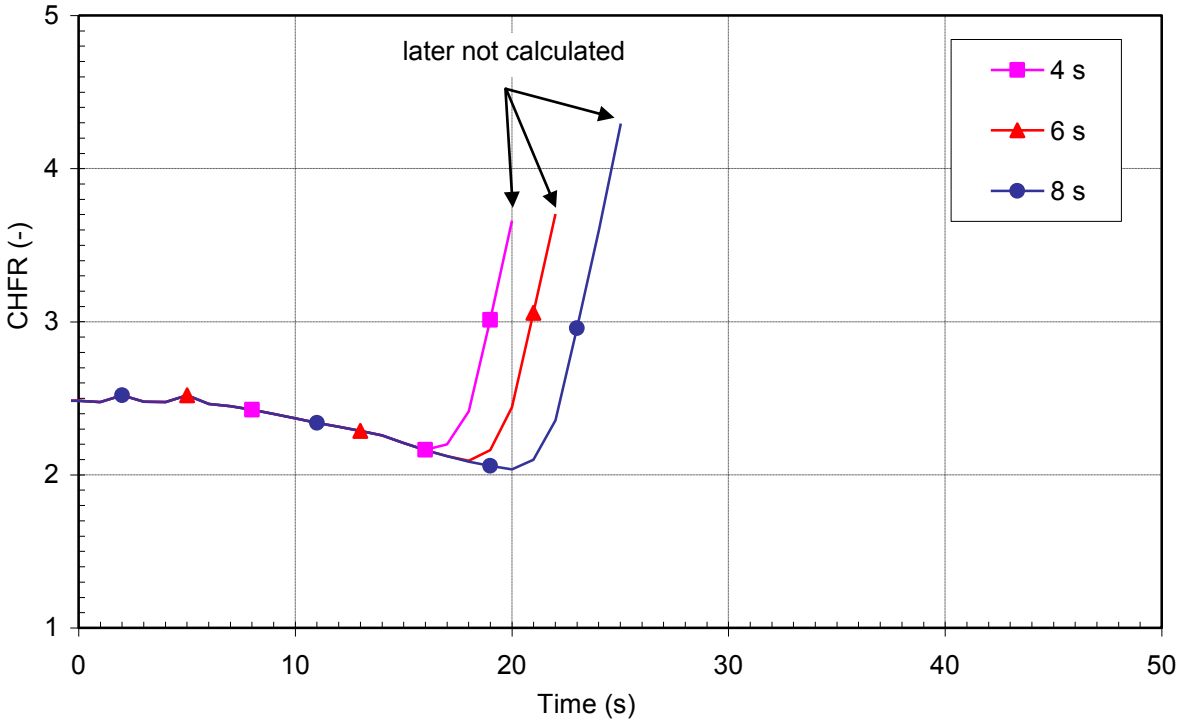

Figure 47 Critical heat flux ratio - influence of measurement delay for case 3

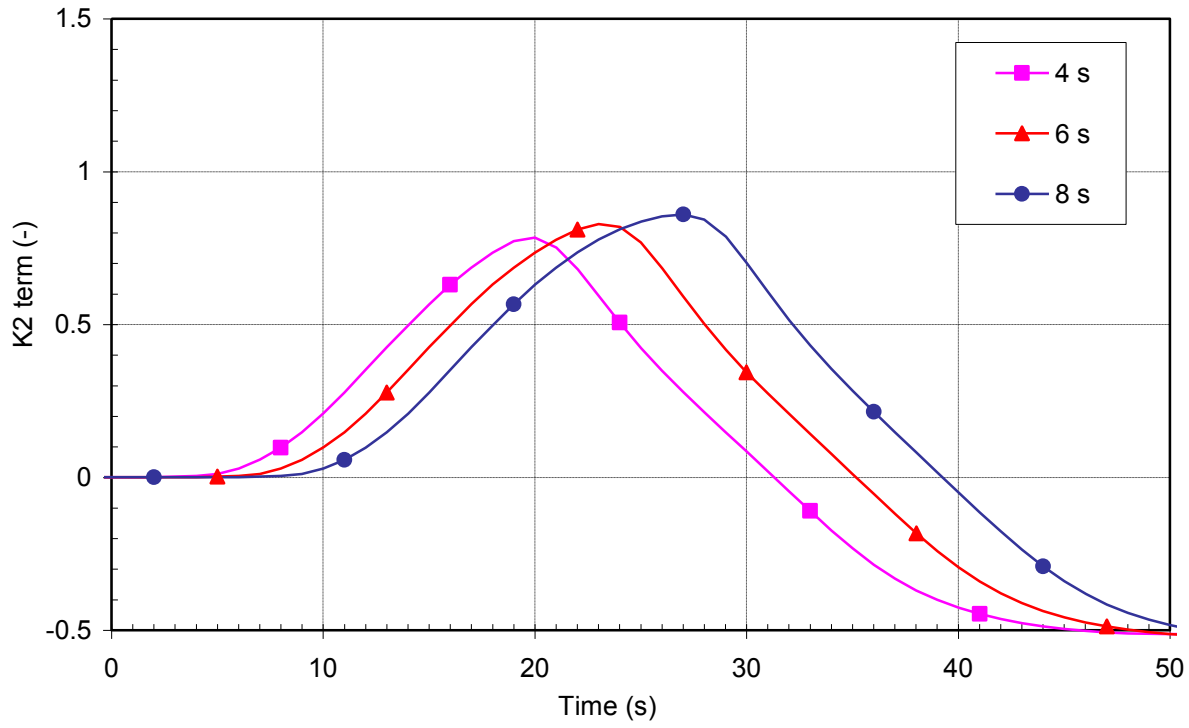

Figure 48 K2 temperature term calculation - influence of measurement delay for case 3

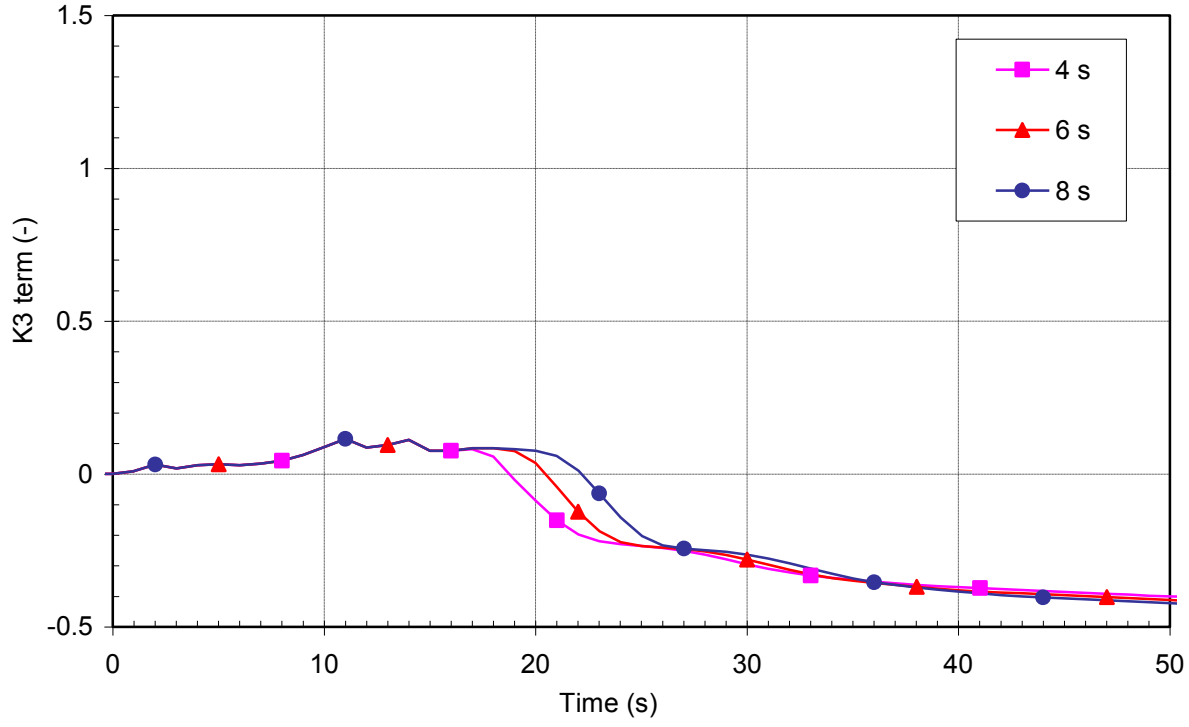

Figure 49 K3 pressure term calculation - influence of measurement delay for case 3

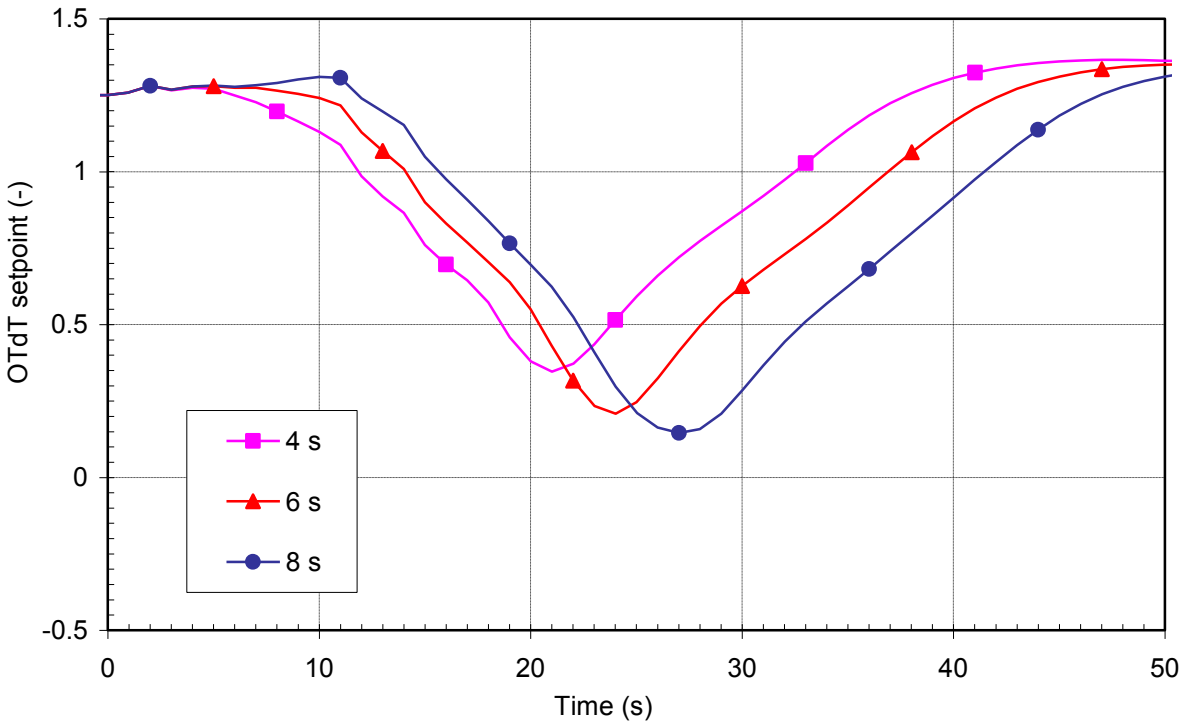

Figure 50 Overtemperature ΔT setpoint calculation - influence of measurement delay for case 3

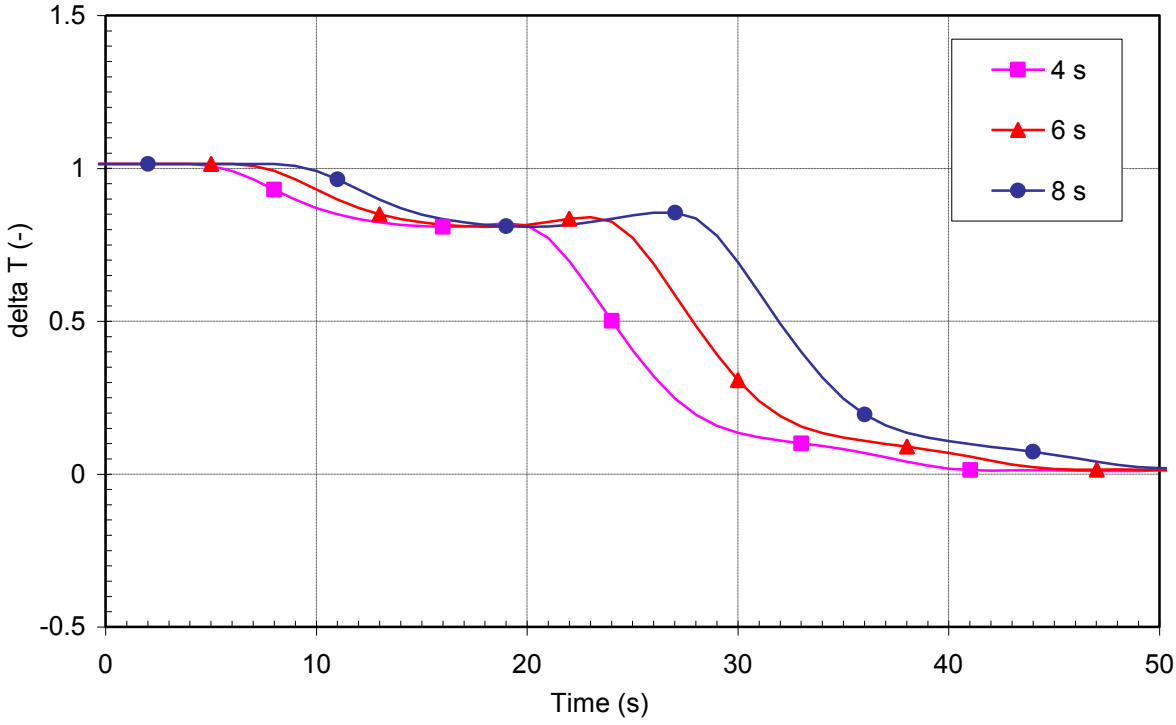

Figure 51 Measured delta T - influence of measurement delay for case 3

5.2.5 Summary of Results

Table 2 shows sensitivity of OTΔT trip time and minimum CHFR on the temperature measurement delay for the three analyzed cases. In addition, the results for base calculation are added. It can be seen that due to disabling high pressurizer pressure and level trips (reactor trip on turbine trip also not assumed by assumption), in all cases the trip times are later due to slower OTΔT protection, causing smaller minimum CHFR than in the base calculation (see Section 5.1). Regarding temperature response time it can be seen that the delay in response almost proportionally delays the reactor trip time on OTΔT. The larger the delay, the smaller the minimum CHFR is. Also it can be seen that in the cases 2 and 3 the primary side cooldown is faster due to best estimate pressurizer sprays and PORVs flow. This minimizes primary pressure what is more conservative for CHFR calculation. On the other hand, also OTΔT trip signal protection responds faster. Finally, Table 2 shows that when comparing cases 2 and 3, the case with smaller RCS flow gives smaller minimum CHFR value.

Table 2 Sensitivity of OTΔT trip time and minimum CHFR on RCS temperature measurement response time

Base calculation (minimum measured RCS flow, reduced pressurizer sprays and PORVs flow)			
Variable			RELAP5 (6 s)
Time of high pressurizer pressure signal setpoint reached (s)			12.56
Minimum evaluated CHFR			2.28*
Case 1 (minimum measured RCS flow, reduced pressurizer sprays and PORVs flow, high pressurizer pressure and level trips disabled)			
Variable	RELAP5 (4 s)	RELAP5 (6 s)	RELAP5 (8 s)
Time of OTΔT signal setpoint reached (s)	16.62	18.51	20.28
Minimum evaluated CHFR	2.18	2.13	2.07
Case 2 (minimum measured RCS flow, best estimate pressurizer sprays and PORVs flow, high pressurizer pressure and level trips disabled)			
Variable	RELAP5 (4 s)	RELAP5 (6 s)	RELAP5 (8 s)
Time of OTΔT signal setpoint reached (s)	15.48	17.22	19.20
Minimum evaluated CHFR	2.13	2.09	2.02
Case 3 (normal RCS flow, best estimate pressurizer sprays and PORVs flow, pressurizer level w/o uncertainty, high pressurizer pressure and level trips disabled)			
Variable	RELAP5 (4 s)	RELAP5 (6 s)	RELAP5 (8 s)
Time of OTΔT signal setpoint reached (s)	15.50	17.31	19.37
Minimum evaluated CHFR	2.16	2.09	2.04

* - at nominal power the CHFR value is 2.48

5.3 Results Discussion

The results show that the selected loss of load transient with multiple failures of reactor protection system trip signals is not the most limiting for the DNB analysis. Based on the CHFR calculations the variations in the initial and boundary conditions and the temperature measurement delay do not much erode the DNBR margin for loss of external load transient. In spite of the fact that CHFR limit was not defined for the RELAP5 lookup tables, the trends between USAR and RELAP5 base calculation are so similar, that sensitivity study to show the influence of measurement delay time could be done based on the CHFR calculations. Having the DNBR trend one may linearly extrapolate the results in the case of larger measurement delays than assumed in safety analysis. The RELAP5 calculations for case 2 show that even when the delay is 8 seconds larger than assumed delay in USAR, the relations are quite linear. Therefore it may be suggested that the presented methodology for CHFR could be used also for other concerned DNB transients relying on OTΔT protection, when informative safety analysis is needed. See Section 1 for explanation why RELAP5/MOD3.3 cannot be used for licensing analysis. For Krško NPP the challenging transient would be inadvertent opening of pressurizer relief or safety valve in which OTΔT protection is slightly faster than would be the low pressurizer pressure trip and the DNB margin is quite small. This means that for a few seconds larger measurement delays the low pressurizer pressure protection signal would be generated before OTΔT. The pressure trend for such transient is linear decreasing function in the case of Krško NPP and also in the case of AP1000 (Ref. 6). For Krško NPP the pressure trend is such that in approximately 2 seconds the pressurizer pressure would fall below the low pressurizer pressure trip setpoint. Nevertheless, in such cases the minimum DNBR limit would be also approached in few seconds. Based on the linear extrapolation of DNBR trend from USAR, up to 4 seconds are remaining. It should be also noted that the OTΔT protection is provided if the transient is slow with respect to piping transient delays from the core to the temperature detectors and pressure is within the range between the high and low pressure reactor trips.

6. RUN STATISTICS

The calculations with the RELAP5/MOD3.3 Patch 03 computer code were performed on a Hewlett-Packard personal computer with Intel Core 2 Quad at 2.40 gigahertz under Microsoft Windows XP, Professional Version 2002, Service Pack 3. Table 3 shows the run statistics for base calculation. For other calculations the statistic is similar, the difference is less than 10%. The differences occur in the period between 10 and 20 s, in which case 1 calculations were the most demanding. For all calculations, the number of volumes was 469. The calculations run faster than real time. Steady-state calculations for all runs lasted 1,000 seconds and required 314.0 seconds of central processing unit (CPU) and 31,427 steps.

Table 3 Run statistics

Transient Time (s)	CPU Time (s)	CPU/Transient Time	Number of Time Steps
25	18.52	0.74	1787
200	73.87	0.37	7185

7. CONCLUSIONS

The analyses of loss of external load were performed using RELAP5/MOD3.3 Patch 03 computer code. The base calculation was performed with the same initial and boundary conditions and assumptions as in the USAR to the extent possible, to demonstrate that RELAP5/MOD3.3 Patch 03 can reproduce the USAR results. Due to non best estimate code used in USAR analysis, the compensation in primary side heatup was made in base calculation to obtain qualitative and quantitative agreement. This was important, because the RELAP5 is limited to calculate the departure from nucleate boiling ratio, which is the safety parameter of interest. It was important to compare the CHFR and DNBR trend in calculation, in which other important parameters quantitatively agree. The trends of CHFR calculated by RELAP5 and DNBR from USAR were similar, while the absolute values were different.

Similar DNBR and CHFR trends makes meaningful to perform sensitivity analysis. The results of sensitivity analysis showed that when the temperature measurement delay is rather small (e.g. ± 2 seconds), the OTΔT trip additional delay is similar to additional measurement delay. The delays impact the curves of important plant variables in such a way that the trend direction is continued for delay time difference and after the reactor trip the curves are time shifted, when compared to each other. As CHFR calculation depends on pressure, mass flux and equilibrium quality, the same is true for CHFR as for these parameters. The larger the measurement delay is, the later the reactor trip on OTΔT is and the smaller the minimal CHFR is. The results also showed that for small delays the relations are linear. It can be concluded that having the DNBR trend from original USAR calculation, one can thus by linear extrapolation of it qualitatively assess how small measurement delay time influence the DNBR during loss of external load. Finally, it should be pointed out that scenarios where three different reactor trips are not functioning besides steam dump and we had to rely on the last reactor protection signal is not much probable and are not analyzed in the safety analysis reports.

8. REFERENCES

1. Ferrouka, M., S. Aissania, F. D'Auria, A. DelNevo, A. Bousbia Salah, "Assessment of 12 CHF prediction methods, for an axially non-uniform heat flux distribution, with the RELAP5 computer code", Nuclear Engineering and Design, 238, 2008, pp. 2718–2725.
2. Parzer, I., B. Krajnc, B. Mavko, "Analyzing Operator Actions During Loss of AC Power Accident with Subsequent Loss of Secondary Heat Sink", NUREG/IA-0225, April 2010.
3. Prošek, A., I. Parzer, and B. Krajnc, "Simulation of hypothetical small-break loss-of-coolant accident in modernized nuclear power plant", Electrotechnical Review, Vol. 71, No. 4: 2004.
4. Parzer, I., B. Mavko, and B. Krajnc, "Simulation of a hypothetical loss-of-feedwater accident in a modernized nuclear power plant", Journal of Mechanical Engineering, Vol. 49, No. 9: 2003.
5. Parzer, I., "Break model comparison in different RELAP5 versions", Proc. of International Conference Nuclear Energy for New Europe 2003. Nuclear Society of Slovenia (NSS), Portorož, September 8-11, 2003. Nuclear Society of Slovenia: Ljubljana, Slovenia. 2003.
6. Westinghouse AP1000-DCD, Westinghouse AP1000 European Design Control Document, EPS-GW-GL-700, Rev. 0.